Fraunhofer
IBMT

FRAUNHOFER-INSTITUT FÜR BIOMEDIZINISCHE TECHNIK IBMT

Thomas Velten (editor)

Roll-to-roll printing of microstructured biocompatible graphene and protein multilayers for biomedical applications

SPONSORED BY THE

Federal Ministry of Education and Research

Innovate UK

M-era.Net

Roll-to-roll printing of microstructured biocompatible graphene and protein multilayers for biomedical applications

Final report of the BMBF joint project M-era.Net - BIOGRAPHY

Dr. Thomas Velten (editor)

Fraunhofer-Institut für Biomedizinische Technik IBMT, St. Ingbert

The work of the German project partners on which this report is based was funded by the German Federal Ministry of Education and Research (BMBF) within the "Innovations for Tomorrow's Production, Services, and Work" Program with the funding numbers 02PN2240, 02PN2241, 02PN2242 and 02PN2243 and supervised by the Project Management Agency Karlsruhe (PTKA).

Part of the project work was undertaken in collaboration with UK partners under the M-ERA.NET, an EU funded network. Furthermore, this project is co-funded by Innovate UK. Innovate UK is the UK's innovation agency. It works with people, companies and partner organisations to find and drive the science and technology innovations that will grow the UK economy.

The responsibility for the content of this publication lies with the authors.

Preface

Biosensors are increasingly relevant for use in medicine and environmental technology, for example, to test new drugs easily and reliably or to be able to quickly detect cell growth in changing environmental conditions. The functionality of the biosensors is based on electrodes on which adherent cell lines are applied. The measured impedance signal changes due to the increased occupancy of the electrodes during cell growth, depends on the measurement task and supplies signals to the electrodes. Due to its catalytic activity, conductivity and biocompatibility, graphene is the ideal electrode material for many biosensors. In order to produce biosensors on an industrial scale using this novel material by means of printing processes, methods for the reliable and automated production of electrode structures and their coating have been developed.

The aim of the joint project M-era.Net BIOGRAPHY was the development of an innovative graphene ink. The ink can be industrially processed into biosensors using a novel printing process on plastic films. Graphene ink was first developed and tested for its biocompatibility, conductivity and printability. A micro-engraving machine was adapted for the fabrication of the required printing cylinders, using a specially focused ultra-short pulse laser. For sensor production, the printing cylinders were integrated into a roll-to-roll printing system. The electrodes produced in this way were tested for their suitability and reliability in cell-based assays to verify the effect of known and novel antiviral drugs.

This innovative production facility made it possible to reliably and automatically print microstructured electrodes that are part of a biosensor. In addition to the analysis and quantification of neutralizing antibody responses for the development of vaccines, these biosensors can also be used in other applications, e.g. in the development of novel antiviral drugs or in cytotoxicity studies. In the transnational funding project M-era.Net BIOGRAPHY, four research groups from Germany worked together with a research group from Great Britain. This cooperation with the foreign partner was essential as it provided the required expertise in the development of a new graphene ink to the German partners.

The German Partners in this joint project were funded by the German Federal Ministry of Education and Research (BMBF) as part of the "Innovations for Tomorrow's Production, Services, and Work" Program. We would like to thank everyone who contributed their knowledge, commitment and experience to this interdisciplinary research and development work.

Projektträger Karlsruhe (PTKA)
Produktion, Dienstleistung und Arbeit
Karlsruher Institut für Technologie (KIT)

Stefan Scherr
July 2018

BIOGRAPHY

Duration:	1st October 2014 – 31st March 2018
Coordinator:	Fraunhofer Institut für Biomedizinische Technik Joseph-von-Fraunhofer-Weg 1, 66280 Sulzbach, Deutschland
Coordinator	**Dr.-Ing. Thomas Velten** Telefon: +49 (0)6897-9071-450 E-Mail: thomas.velten@ibmt.fraunhofer.de
Project partners and authors	Fraunhofer Institut für Biomedizinische Technik (IBMT) Joseph-von-Fraunhofer-Weg 1, 66280 Sulzbach, Deutschland *Dr. Thomas Velten, Thorsten Knoll, Dr. Anke Schultz* SAUERESSIG GmbH + Co. KG Gutenbergstrasse 1-3, 48691 Vreden, Deutschland *Dr. Gerald Jenke, Renate Warmers, Dr. Anna Zumbülte* AiCuris Anti-infective Cures GmbH Friedrich-Ebert-Str.475, 42117 Wuppertal, Deutschland *Dr. Andreas Urban* cellasys GmbH - R&D Ohmstrasse 8, 80802 München, Deutschland *Dr. Joachim Wiest* Haydale Limited Clos Fferws, Parc Hendre, Capel Hendre, Ammanford, Carmarthenshire, SA18 3BL, United Kingdom *Dr. Kris Seunarine, Dr. Neil Vyas, David Davies*

Content

1 Objectives and consortium 7

1.1 Objectives of the research project 7

1.2 Consortium 7

2 State of the art at the beginning of the project 9

2.1 State of the art in the targeted biotechnological fields of application 9

2.2 State of the art in the targeted production techniques and in the field of printed electrically conductive microstructures 9

2.3 State of the art in the production of printing cylinders for rotary gravure printing 11

3 Results 12

3.1 Selection of microstructures 12

3.2 Process for microstructuring of printing cylinders 13

3.3 Biocompatible graphene ink suited for roll-to roll printing 15

3.3.1 Graphene ink 15

3.3.2 Biocompatibility testing 16

3.4 Roll-to-roll processes for multifunctional surface coating of foils 20

3.4.1 Graphene printing 20

3.4.2 Protein coating of graphene electrodes 23

3.4.3 Two-colour gravure printing 23

3.5 Evaluation of surface functionalised foils for sensor applications 24

3.5.1 Set-up of printed impedance sensors for validation of antiviral substances 26

3.5.2 Virus-induced cytopathic effect and its inhibition 28

3.5.3 Cytopathic effect at different virus concentrations 31

3.5.4 Cytopathic effect depending on infectivity of viruses 34

3.5.5 Set-up of printed sensors for toxicology 36

3.5.6 Evaluation of printed impedance sensors for validation of antiviral substances 37

3.5.7 Evaluation of printed sensor for toxicology 40

3.6 Production line for roll-to-roll surface functionalization of foils by two-colour-printing 42
4 Summary of results and possible applications 46
4.1 Summary of the results 46
4.2 Possible applications 46
5 Acknowledgement 48
6 List of references 49

1 Objectives and consortium

1.1 Objectives of the research project

The BIOGRAPHY project aims at developing a highly efficient production line and process for the roll-to-roll printing of graphene-based, multi-functional microstructures on large-area polymer foils, the process thus being suited for the mass production of highly innovative biosensors.

In brief the project objectives are as follows:

- Development of a biocompatible, electrically conductive graphene ink being suited for gravure printing. High conductivity inks usually contain inorganic elements not suitable for contact with living cells. Organic inks currently available lack the conductivity required to provide a high performance sensor. The recent availability of a variety of graphene will enable the conductivity of a fully organic biocompatible ink to meet both the electrical conductivity requirement and the biocompatibility needs. This will require the identification, functionalisation and formulation of appropriate graphene and organic combinations and the development of suitable carriers appropriate to both the product and the printing method.
- Establishment of a fabrication method for large area micro patterning of gravure printing cylinders. We aim at a lateral pattern resolution of < 10 µm.
- Establishment of a roll-to-roll process as well as a two-colour printing roll-to-roll production line for surface functionalisation of large area polymer foils. Functionalisation will be done by gravure printing of a micro-patterned graphene/protein multilayer. Challenging issues, especially with regard to the small printing structures, are the correct adjustment of printing parameters, adjustment of surface energies of ink, printing cylinder and corona-activated polymer foil in order to achieve perfect filling and emptying of printing cells and perfect pattern transfer for both, graphene ink and protein ink. The graphene layer is electrically conductive; the protein layer ensures a good cell adhesion. It is challenging to find suited process parameters to guarantee a sufficiently rapid drying of the graphene ink in order to avoid that graphene and proteins do mix in an unacceptable manner.
- Evidence of the suitability of the printed graphene/protein coating for sensor applications. As an example, we proof the suitability of the printed graphene/protein micro patterns for application in vaccine and antiviral drug validation. To this end, we develop a printed impedimetric sensor and show that it is suited for online monitoring of the virus-induced cytopathic effect (CPE) in cells for virus detection. Achieving this objective is very challenging because the printed graphene electrodes and electronic conducting paths need to be highly conductive in order to achieve a good sensor resolution. In addition, the inhibition of the CPE in the presence of neutralizing antibodies will be monitored for the intended utilization for the validation of vaccines in neutralizing antibody assays. Furthermore, we validate the suitability of the printed coatings for applications in cell based toxicity tests.

1.2 Consortium

The project consortium comprised five partners, four from Germany and one from the UK. Cross-border cooperation under the MNT ERA-NET, a network of regional and national micro

and nanotechnologies funding organizations in Europe, with British project partners, provided access to the development of new microfabrication technologies and to new conductive inks. Specifically, the British project partners developed a graphene ink suited for rotogravure printing.

Within the project, the Fraunhofer IBMT selected graphene and protein microstructures to be printed, developed process parameters to print graphene and proteins by gravure printing and verified the biocompatibility of both the graphene ink and the printed structures. Furthermore, impedimetric biosensors were set up and partner AiCuris was assisted in sensor validation. The main focus of IBMT's validation activities were related to virus detection and the assessment of the efficacy of vaccines (while AiCuris' activities focused on antiviral drugs).

SAUERESSIG developed methods to engrave gravure printing cylinders with smaller structures than it was possible before. Gravure printing cylinders were structured according to guidelines provided by Fraunhofer IBMT and cellasys. Structured cylinders were provided to project partner Fraunhofer IBMT. In several iteration steps, based on the print results obtained, the structures were adjusted so that optimum printing results even at sub-10 microns structures could be achieved.

Based on the printed results obtained at Fraunhofer IBMT as well as on the in-house know-how in the field of roll-to-roll production, SAUERESSIG built a production line that is capable of surface functionalization with graphene and proteins in a single roll-to-roll process.

Haydale developed a new graphene ink which is a) biocompatible, b) produced in an environmentally friendly manner, c) electrically conductive, d) suited for rotogravure printing.

AiCuris checked the suitability of the developed surface functionalization processes and production line for applications in antiviral drug development. Specifically, this was done by means of a) detection/monitoring of the virus-induced CPE (cytopathic effect) of viruses into cells and b) detection/monitoring of the inhibition of this effect mediated by antiviral substances. For this purpose the cells were located on the printed electrodes which were further functionalized with a printed micro-structured protein layer for improving cell adhesion. Detection and monitoring were done by online impedance measurements.

cellasys adapted the design and materials of an already existing impedance-type micro sensor to the capabilities of the roll-to-roll surface functionalization process envisioned within BIOGRAPHY for a single chip version and for a 24 well plate version. The substrate was further functionalized with hepatocytes in order to obtain a complete cell-based biosensor. Biosensors realized in this way were evaluated for usage in repeated dose toxicological applications.

2 State of the art at the beginning of the project

2.1 State of the art in the targeted biotechnological fields of application

The induction of neutralizing antibody responses after vaccination plays an important role in the immunization against viral infection and has been successfully implemented in numerous viral diseases such as smallpox, measles or polio. The main effector function consists of the extracellular neutralization of the viruses, whereby the surface receptors necessary for the infection of a host cell are bound and thus masked, which prevents the infection of the target cell. The analysis of neutralizing anti-body responses after vaccination thus is an essential part in the evaluation of the efficiency of a new vaccine. In neutralization tests, the biological function of the antibody responses can be determined in vitro, which in particular provides information about the quality of the antiviral substances. Such state-of-the-art neutralization tests are also used at the Fraunhofer IBMT.

Especially in the field of neutralization assays for evaluating the efficiency of vaccines, today's methods are expensive and dependent on complex experimental procedures as well as additional detection systems (e.g. reporter genes and viruses). Therefore, simple and cost-effective methods are of particular interest since they would lead to an immense cost reduction in vaccine development in the area of quantification of neutralizing antibody responses in cell-based neutralization tests and the identification of new antiviral substances. Furthermore, it would be desirable to have methods which not only display the final result at a fixed point in time, but also acquire measured values virtually continuously. Like this it would be possible to record the time course of the test and also to offer the time-saving possibility of terminating the test immediately when a meaningful result is available.

2.2 State of the art in the targeted production techniques and in the field of printed electrically conductive microstructures

Electrically conductive inks already existed before the project start. These inks were mainly developed for applications in the field of printed polymer electronics. Organic conductive inks have been prepared, but have low electrical conductivity due to low mobility of the charge carriers (e.g. <0.5 $cm^2V^{-1}s^{-1}$ [1]). To improve the conductivity, electrically conductive nanoparticles were also used, such as polysilicon [2], zinc oxide nanoparticles [3], or carbon nanotubes [4]. However, metal nanoparticle-based inks are not stable in typical solvents such as deionized water, acetone or isopropanol [5]. Therefore, they must be chemically modified by means of suitable stabilizers. These stabilizers are not long-term stable, and the metal nanoparticles also begin to oxidize after printing [6].

Charge carrier mobilities of up to 50 $cm^2V^{-1}s^{-1}$ have been achieved with electrically conductive inks based on carbon nanotubes [7]. With graphene-based inks even a mobility of 95 $cm^2V^{-1}s^{-1}$ has been achieved [8]. These graphene inks were not developed for rotary printing, and not for biomedical applications, but for ink jet printing of electronic circuit traces.

Initial development toward graphene ink suitable for both biological applications and for roll-to-

roll printing is described in [9] and was carried out at the University of Maryland, USA.

Commercial graphene-based inks were few at the beginning of the project, and existed especially in the US and the Far East. VorbeckMaterials (USA) offers graphene ink, but it has been developed for battery applications and not for biomedical applications. In addition, the Thai company INNOPHENE offers a graphene ink. According to INNOPHENE's corporate homepage, graphene inks are available for screen printing, roll-to-roll printing and inkjet printing.

In Europe, there were few, perhaps even just one single commercial graphene ink supplier, the British BIOGRAPHY project partner Haydale Ltd. The graphene ink from Haydale Ltd. was developed for the screen printing process and was not tested for biocompatibility. For roll-to-roll printing processes and for biosensor applications, the graphene ink from Haydale Ltd. was not suitable before the start of the project.

In Europe, there was a need to catch up with graphene inks which are suitable for roll-to-roll printing processes and / or which have the biocompatibility required for biomedical applications.

Roll-to-roll printing is a well-known process for cost-effective printing of patterns on surfaces in large quantities. Mainly the rotogravure printing is applied. Rotogravure printing cylinders have small holes etched into the printing cylinder which define the print pattern. The holes are filled with a dye solution, which is transferred during rotation of the printing cylinder on an endless roll of paper or plastic.

In addition to the standardized roll-to-roll printing process for printing inks, there were also first methods for realizing electrically conductive microstructures in roll-to-roll processes. These methods are usually unsuitable for use in biomedical applications because the employed materials and methods are not biocompatible. For example, research activities on printed electronics took place at Fraunhofer IISB. Here, metallization was realized by means of the conventional sputtering technique. In addition, there existed a method of printing conductive inks by means of an inkjet printer. These research activities focused on the purely technical field of "printed electronics", in which the biocompatibility of the used materials - as required in biomedical applications - does not matter.

First methods for the realization of simple diagnostic microsystems in the roll-to-roll method already existed in the field of diagnostics. Roche Diagnostics realizes electrode structures by microstructuring a film coated with metal over the whole area in a roll-to-roll process by means of laser ablation. However, the structure resolution and the process speed are subject to some limitations and are for example not suitable for the realization of interdigital electrode arrays with a few micrometers electrode width, as they are needed for some electrochemical biosensors.

Commercial use of rotary printing methods, such as e.g. gravure printing, for the production of printed electrically conductive structures was little known at the beginning of the project. A company active in this field is PolyIC, which specializes in the production of printed electronics and therefore does not need to use biocompatible materials.

The printing of biocompatible conductive graphene layers in the roll-to-roll printing process was, to our knowledge, not used commercially at the beginning of the project. Similarly, roll-to-roll printing of a biocompatible multifunctional graphene / protein bilayer was not state of the art.

2.3 State of the art in the production of printing cylinders for rotary gravure printing

Today's technologies for micro patterning of commercially used gravure printing cylinders are limited to > 10 µm, usually even to > 20 – 30 µm. Those printing cylinders feature small depressions into the surface – so called printing cells – presenting the printing design. In the printing process the printing cells are filled with ink and the ink is transferred to the substrate.

There are mainly three standard processes to produce gravure printing cylinders:

1) Electromechanical gravure: A diamond graver oscillates and engraves the printing cells into the cylinder surface.
2) Laser/etching: Like in lithography a mask covering the cylinder surface is structured by a laser. Afterwards the cylinder is etched and the mask is removed.
3) Direct lasing: A laser directly creates the printing cells in the cylinder surface.

A technology for realizing structures < 10 µm in printing cylinders would be beneficial for printed sensors, but also for other applications like printing of security features e.g. on banknotes.

3 Results

The project BIOGRAPHY was divided into the following work packages:

WP1: Selection of microstructures for functionalization of graphene based printed biosensors
WP2: Process for microstructuring of printing cylinders
WP3: Biocompatible graphene ink suited for roll-to roll printing
WP4: Roll-to-roll processes for multifunctional surface coating of foils
WP5: Evaluation of surface functionalised foils for sensor applications
WP6: Production line for roll-to-roll surface functionalization of foils by two-colour-printing (graphene ink, immediately followed by protein ink)

The results achieved during the project duration are presented in the following sub-chapters.

3.1 Selection of microstructures

Printed interdigitated electrode structures will be used for all impedimetric sensors. For the application in online monitoring of the virus-induced cytopathic effect in cells electrode structures were specified to monitor both, morphological changes and proliferation of cells via impedance measurement. A 96-well plate format has been selected for this application. 24 out of the 96 wells are equipped with electrode structures and can be used for performing measurements (Figure 1).

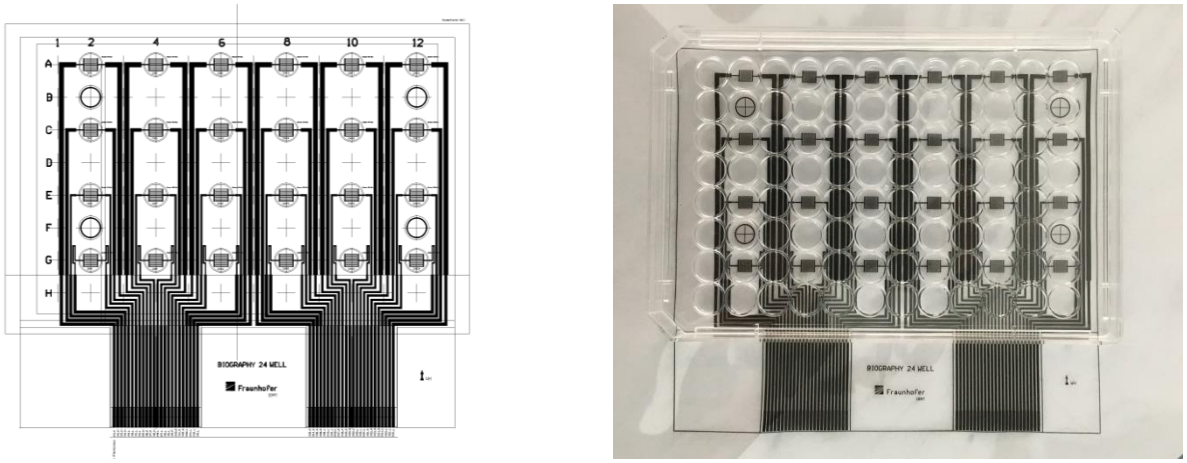

Figure 1: Arrangement of the 24 interdigitated electrode structures within a 96-well plate. Left: Schematic presentation of interdigitated electrodes, tracks and electrical contacts. Right: Printed structure covered by the lid of a 96-well plate to demonstrate positions of wells and electrode structures.

For the application in toxicology the use case of repeated dose application of chemicals toward hepatocytes was selected. The micro structured electrodes were specified to monitor morphological changes of cells via impedance measurement and to be available in two different set-ups (a single chip version and a multiwell plate version). Figure 2 depicts the layouts of the different set-ups, as well as the realization.

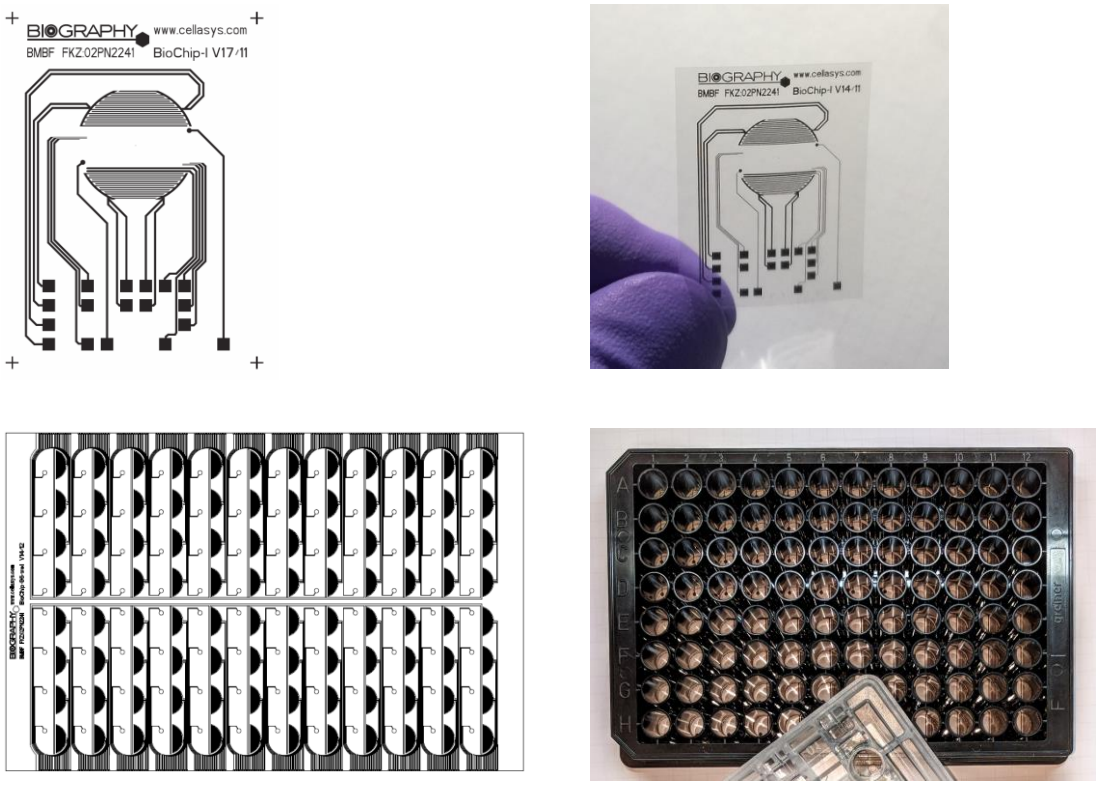

Figure 2: BioChip-I (top) with dimensions 24 x 36 mm² and BioChip-96-well (bottom) with dimensions 127 x 85 mm².

To optimize the design of the interdigitated impedance structure a protocol for measurement with and without living cells was developed and the optimal structure was defined to be 100 µm width of the finger and 100 µm distance. The results were presented at the 39th Annual International Conference of the IEEE Engineering in Medicine and Biology Society [10].

3.2 Process for microstructuring of printing cylinders

A new laser-based micromachining method for the production of gravure cylinders was developed. The microstructures in the gravure cylinder were generated by direct ablation of the metal surface by a picosecond laser. The pulses of this laser are so short that the metal is directly sublimated. In order to achieve the required lateral feature sizes of < 10 µm the engraving machine had to be equipped with optimized focusing optics. Afterwards the optimal laser parameters had to be evaluated in several preliminary tests. Besides the pulse duration and the pulse frequency especially the power of the laser source and the modulation play a decisive role. In addition the surface speed and the feed had to be optimized.

With these new components and adjustments the first gravure printing cylinder for proteins was produced. The design of the cylinder was based on the knowledge from the previous Era-net project 'BIOREEL' as well as on the results of work package 1. The design consists of areas with regularly arranged dots with several diameters in the range of 5 to 50 µm. The depth of the dots was varied between 7 and 11 µm. Both the diameter and the depth of the microstructures

should be reduced for the following printing cylinders. The protein transferring dots were arranged over the whole circumference and the whole width of the cylinder. Hence it could be used as a first test for protein printing in combination with several graphene printing cylinders. Figure 3 shows two parts of the cylinder surface.

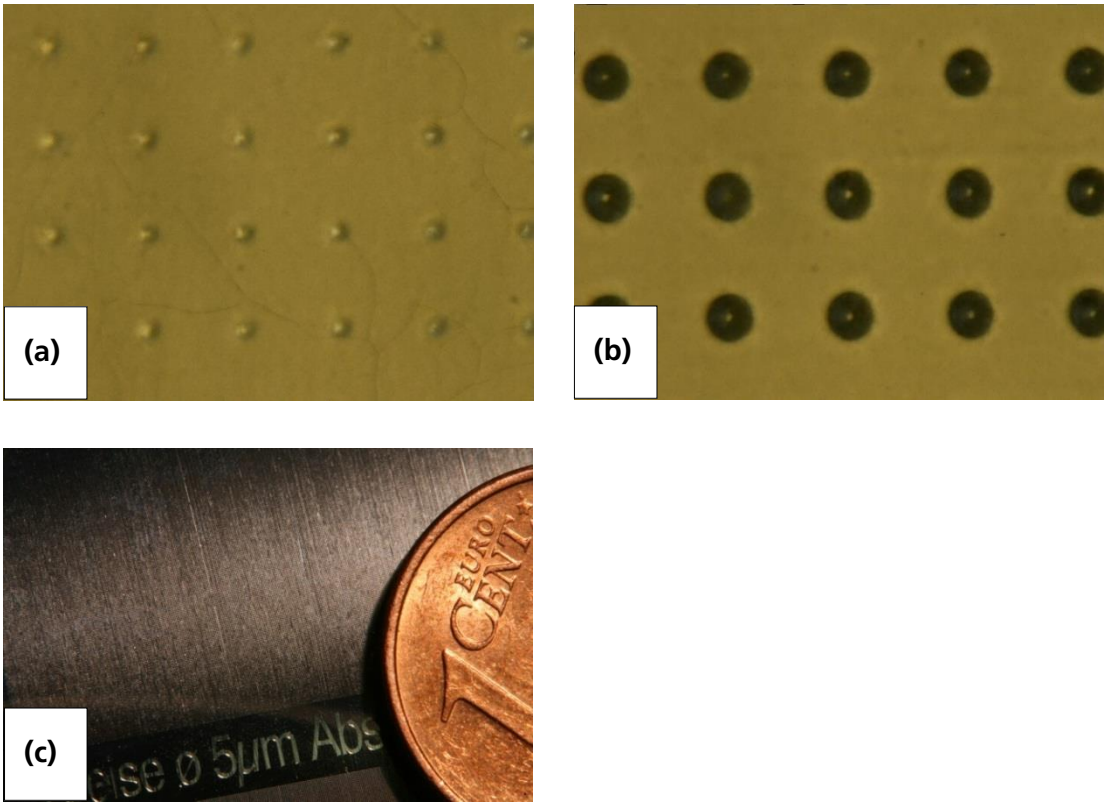

Figure 3: Microstructuring for proteins; (a) dot diameter 9 µm, (b) dot diameter 26 µm, (c) PDMS replication of microstructures with dot diameter 5 µm.

During the first printing experiments it turned out that the cell growth was insufficient because the amount of the transferred proteins to the polymer film was not high enough. For this reason the original plan of using microstructures had to be dropped. Instead, a printing cylinder with bigger structures was produced to increase the amount of proteins on top of the graphene structures. Prior to production the design and the parameters of the graphene printing cylinder had to be defined and optimized (see multiple consecutive designs in work package 4 described in chapter 3.4).

Based on the final graphene printing cylinder layout the design of the cylinder for protein printing was defined. Both designs are shown in Figure 4. A continuous area of proteins should be printed over the graphene finger structures to ensure the maximum possible amount of transferred proteins in these regions.

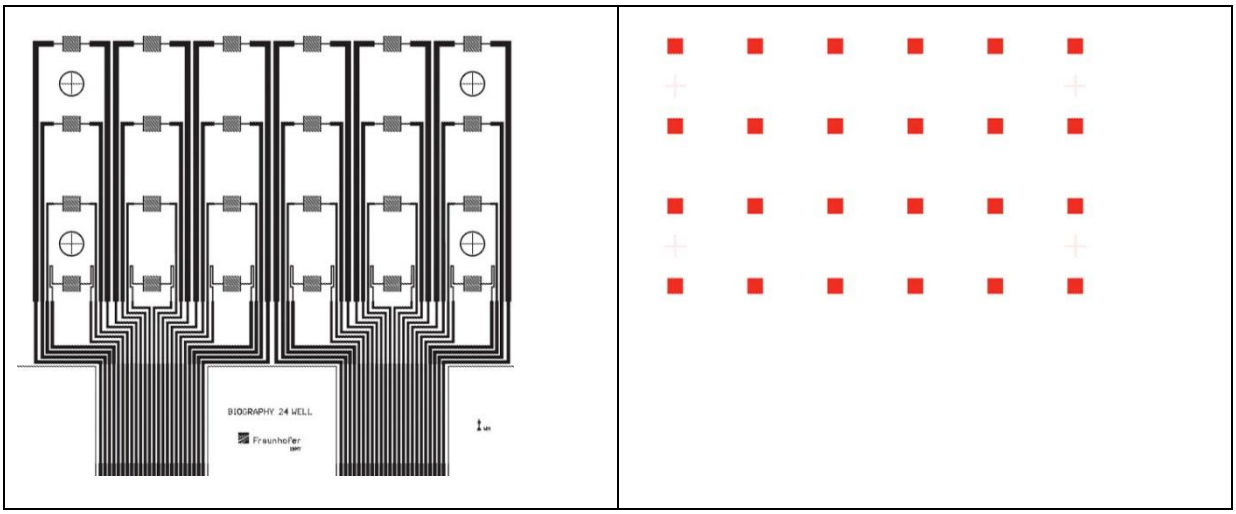

Figure 4: Design of printing cylinders. Left: Design of IBMT 24-well plate for graphene ink. Right: Design of IBMT 24-well plate for protein ink.

3.3 Biocompatible graphene ink suited for roll-to roll printing

3.3.1 Graphene ink

Graphene enhanced ink for biosensing application has two major advantages over other non-graphene-based materials. This includes biosensors based on graphene do not contain metallic impurities which may interfere electrochemically with the test samples. Furthermore, graphene can be easily attached to most biomolecules by π – π stacking due to its biocompatible nature.

The graphene-enhanced ink developed by Haydale is electrically conductive and biocompatible as a printed layer. Due to graphene's one atom thick 2D planar structure and high surface-to-volume ratio, the ink is highly sensitive towards chemical changes in the surrounding environment which is an important advantage in terms of biosensing application. All carbon atoms in graphene-based ink interact directly with the analytes providing higher sensitivity than silicon nanowires or CNT based sensing devices. Biocompatibility of graphene-based ink was demonstrated in cytotoxicity tests according to ISO 10993-5 with different cell lines. The ink was modified such that it could also be applied through rotary gravure printing producing printed structures with significantly low surface resistance of 10 Ω/sq based on a layer thickness of 25 µm. A laser equipped micro-engraving machine was used to produce gravure cylinders in this case which was capable of printing electrically conductive tracks with lateral dimensions less than 100 µm. In addition, the ink needed to be formulated to have suitable viscosity and fast drying so that an accurate printing at high speed and with good definition can be achieved.

Haydale graphene enhanced ink is composed of three main component types: Resin (or binder), solvents and additives such as pigments or other functional additives. The combination of targeted properties was made possible by careful and considered selection of the constituents, specifically the addition of Haydale's Graphene Nanoplatelet (GNP) material as a key active ingredient. The ink was formulated using a variety of mixing and dispersion methods; GNPs were mixed into the resin vehicle, and then put through a series of compounding procedures to ensure adequate uniformity through the ink. GNPs are high-aspect ratio carbon nanomaterials

which are processed and surface-functionalized using Haydale's patented HDPlas® plasma-based technology. The plasma functionalization process promotes efficient dispersion into the carrier resin used in the ink; it is this effective dispersion that allowed the ink to more readily exhibit the desired characteristics described above.

The low energy HDPlas® process is able to add functional chemistry in a uniquely benign manner, which causes very minimal damage to the nanomaterial structure, thereby maximizing the ability to impart the nanomaterial properties to the final ink. HDPlas® technology takes full advantage of the planar structure and unique chemical properties of graphene for incorporating additional functional groups on the surface of the material. This leads to a range of application specific surface engineered GNP materials with various advantageous properties compared to other nanomaterials for biosensing applications.

Some of these project results were made public by Haydale Limited in a press release, using in part the same wording [11].

3.3.2 Biocompatibility testing

The biocompatibility of the graphene ink was validated according to DIN ISO 10993-5 ("Biological evaluation of medical devices"). This was performed by utilizing three different methods: (i) the WST-1-test; (ii) the BrdU-test and (iii) the live / dead staining of the cells. The first two procedures are indirect and quantitative techniques: The WST-1-test determines the metabolic activity in form of an active respiratory chain, while the BrdU-test determines the rate of cell division. The samples of interest (see following paragraph) were incubated for 24 h with the culture medium to generate the extracts for the biocompatibility testing. The live / dead staining is a qualitative direct contact test, where the indicator cell line was grown for 48 h directly on the graphene samples. The viable cells were stained using fluorescein diacetate (FDA) and appeared as green fluorescent cells. The dead cells were stained with propidium iodide (PI) and appeared as red fluorescent cells. As defined for biocompatibility tests the human fibroblast cell line MRC5 was used as indicator cell line for the procedures described above.

Different samples were analysed within this biocompatibility study: (i) The PET-foil substrate (PET) as biocompatible reference material, (ii) the Haydale graphene ink pure (GP), (iii) the Haydale graphene ink plus acetone as solvent (GA), (iv) the Haydale graphene ink plus DMSO as solvent (GD) and (v) the Haydale graphene ink plus diacetone as solvent (GDA). In Figure 5 two examples of testing material are depicted, the PET foil and an example with a screen printed pure graphene ink on the foil substrate. The PET foil as well as the printed one with the graphene ink and the respective utilized solvent were analysed after the sterilization with ethylene oxide.

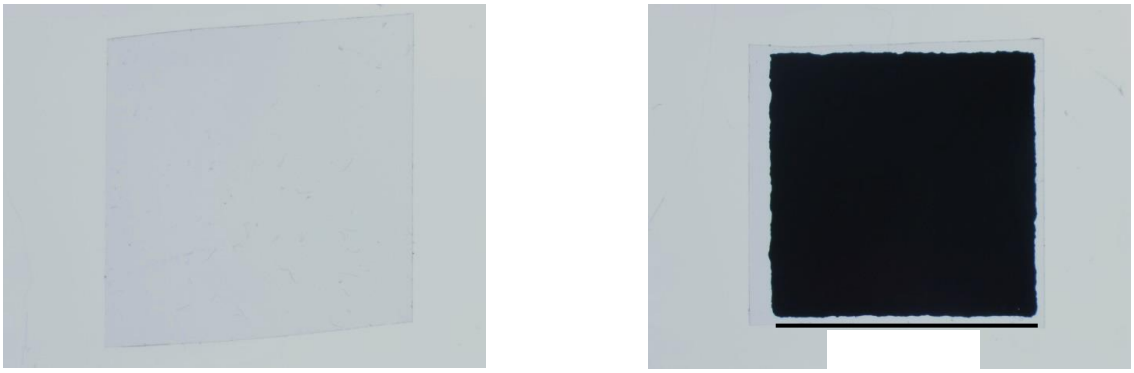

Figure 5: Examples of the test material used for the biocompatibility testing. Left: Bare PET foil. Right: Screen printed pure graphene ink (Haydale) on the PET foil.

The microscopic evaluation after 24 h incubation of the MRC5 cells with the extract of the different printed foil substrates revealed no morphological changes (Figure 6). This result was also confirmed with the WST-1 and BrdU-test (Figure 7). A high metabolic activity and cell proliferation (nearly 100 %) was detected for all tested samples. The printed graphene ink dissolved in diacetone showed a slight reduction in the relative growth rate in the WST-1 test. This might be due to a slower evaporation behaviour of the diacetone. This could be reduced by additional washing steps with medium before the initiation of the extraction procedure in further analysis. However, this does not change the general findings that, by using the quantitative testing procedures, the tested Haydale ink samples added with different solvents were verified as biocompatible.

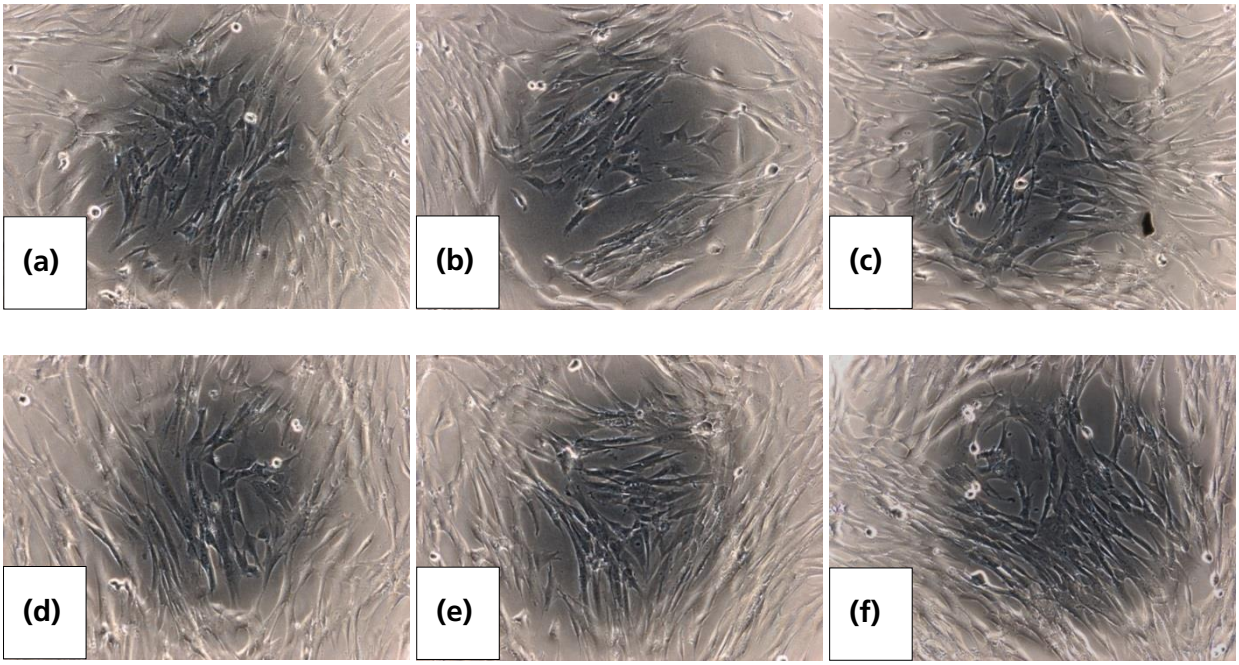

Figure 6: Microscopic view of the MRC5 cells after 24 h incubation with the cell extracts: (a) Control (polystyrene plates suited for cell culture), (b) PET foil, (c) pure graphene ink, (d) graphene ink plus acetone, (e) graphene ink plus DMSO, (f) graphene ink plus diacetone.

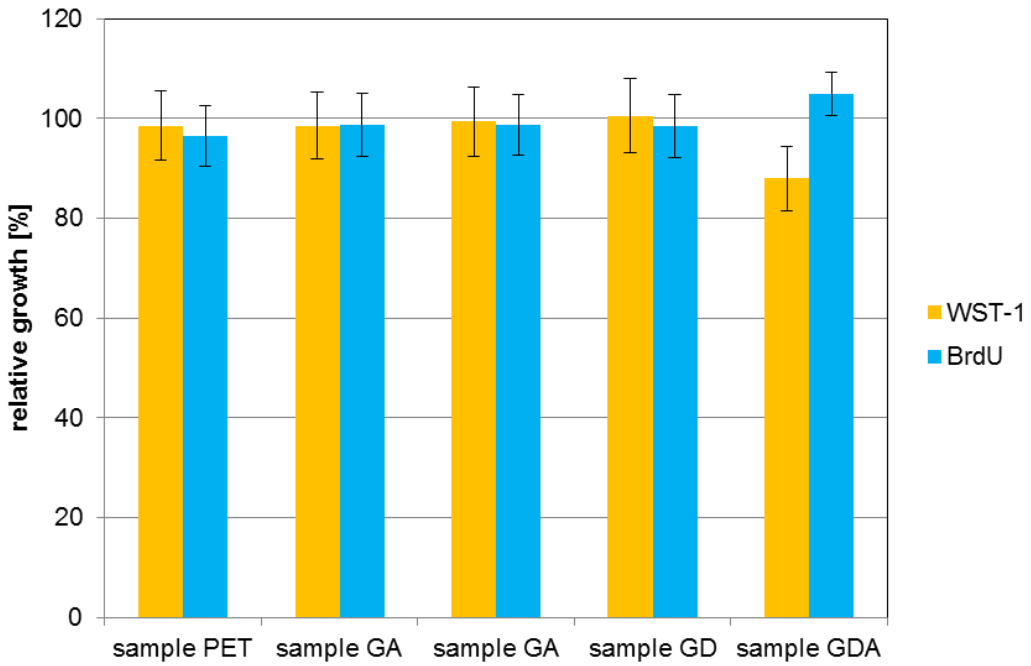

Figure 7: Illustration of the indirect quantitative WST-1- and BrdU-test as relative growth in % after incubation of the MRC5 with the extracts of the different foil substrate samples.

In addition, the results of the direct contact test demonstrated that 48 h after seeding of the MRC5 cells on the foil substrate samples no cell cytotoxicity was observed. The cells grew on the printed areas and showed a good viability (green fluorescence) with nearly no dead cells (red fluorescence) on the samples. However, compared to the control of the polystyrene plate the cell number was reduced and the cell morphology changed (Figure 8).

This rose the question, if the adherence of the cells could be enhanced by coating the graphene printed foil substrates with 1 ml protein solution for 4 h at 37 °C. Within this experiments Collagen type IV from human placenta (Molecular Probes) or Matrigel, a basement membrane preparation of the Engelbreth-Holm-Swarm (EHS) mouse sarcoma, a tumor rich in extracellular matrix proteins (Corning) was utilized as coating material. Figure 9 clearly demonstrates that the protein treatment led to an improvement of the cell number and the morphological shape of the MRC5 cells on the graphene surface on the foil substrate. This was shown for the pure graphene ink as well as for the ink dissolved with diacetone.

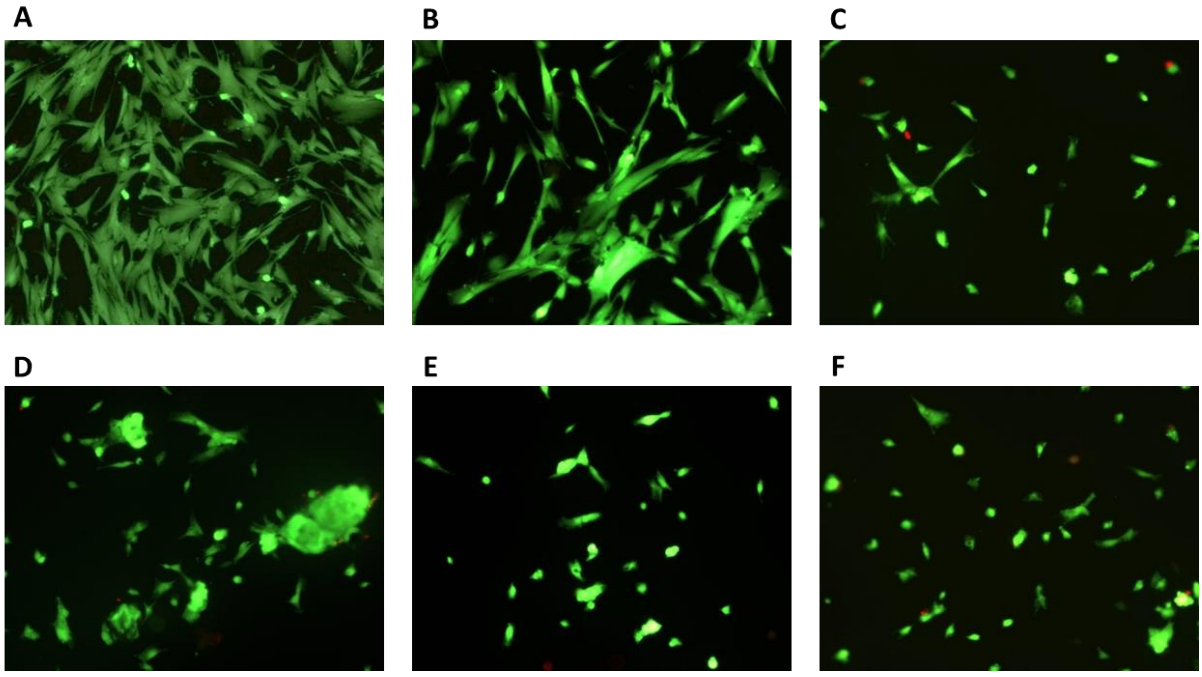

Figure 8: MRC5 cells 48 h after seeding on the foil substrates without and with graphene: (A) Control (polystyrene plates suited for cell culture), (B) PET foil, (C) pure graphene ink, (D) graphene plus acetone, (E) graphene with DMSO and (F) graphene plus diacetone. Green cells correspond to FDA-stained viable cells and red cells to PI-stained not viable ones.

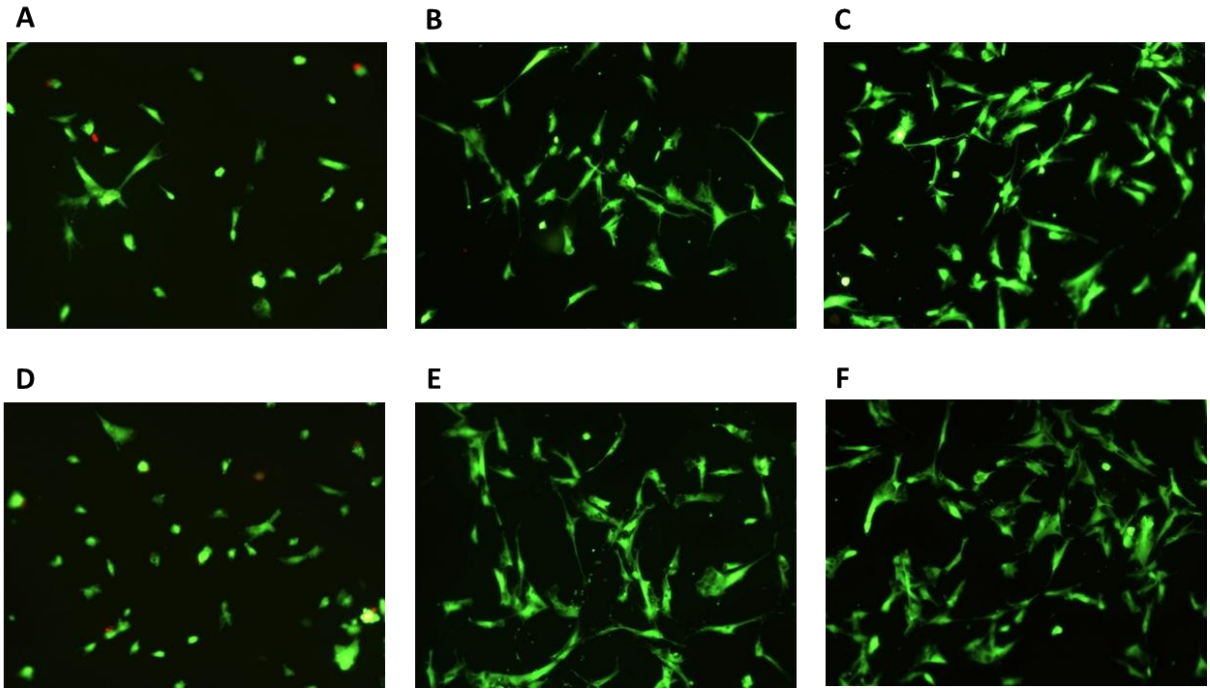

Figure 9: MRC5 cells 48 h after seeding on the foil substrates plus graphene coated with different protein solutions: (A) Pure graphene ink, (B) pure graphene ink plus Collagen type IV, (C) pur graphene ink plus Matrigel, (D) graphene plus acetone, (E) graphene plus diacetone plus Collagen type IV and (F) graphene plus diacetone plus Matrigel. Green cells correspond to FDA-stained viable cells and red cells to PI-stained not viable ones.

In conclusion, the biocompatibility of the graphene ink was validated successfully for the pure graphene and for the graphene dissolved in acetone, DMSO or diacetone. The results concerning ink development and cytotoxicity testing were presented at the Advanced Functional & Industrial Printing conference (AFIP 2016) [12] and published in the Proceedings of The Global Conference on Micro Manufacture (4M/IWMF2016) [13]. However, the adherence of the MRC5 fibroblasts on the graphene ink was reduced. This obstacle was overcome by coating the graphene-printed PET foil substrates with proteins. So, besides the principle suitability of the Haydale graphene ink as basis for setting up sensors for impedance measurement, the outcome of the above described tests emphasize the requirement to additionally coat the foil substrate with a protein layer.

3.4 Roll-to-roll processes for multifunctional surface coating of foils

3.4.1 Graphene printing

Various graphene inks from Haydale were diluted with solvent immediately before printing, then printed and characterized for their printability (structure fidelity and layer thickness) and electrical resistance. Nine different graphene inks were tested, which differed mainly in the number of milling steps of the graphene flakes and in the concentration of the solvent. Furthermore, inks with reduced resin content were examined. The latter proved to be less resistant to abrasion and led to significantly higher layer thicknesses compared to all other investigated inks. Despite the higher layer thicknesses, the electrical resistance was about two to three times higher than for inks with "usual" resin content. We suspect that the inks with reduced resin content result in a relatively porous structure with low density. Therefore, the printed layers are not very abrasion-resistant and the graphene flakes have few points of contact and therefore cannot conduct the electric current very well from flake to flake.

The thicknesses of the graphene layer achieved by gravure printing only varied slightly between the different types of graphene ink. The only exception was the previously mentioned ink with reduced resin content. The depth of the wells of the gravure printing cylinder had a major influence on the layer thickness. There was an approximately linear relationship between the layer thickness and the well depth. At a well depth of 80 µm, the layer thickness was about 4 to 5 µm.

We also printed graphene test patterns that were suitable for measuring the square resistances of printed graphene layers. The conductivity of the printed test structures correlated largely with the number of milling steps of the graphene ink used (Figure 10). Some of the examined graphene inks achieved a square resistance of < 10 Ω/square (normalized to a layer thickness of 25 µm).

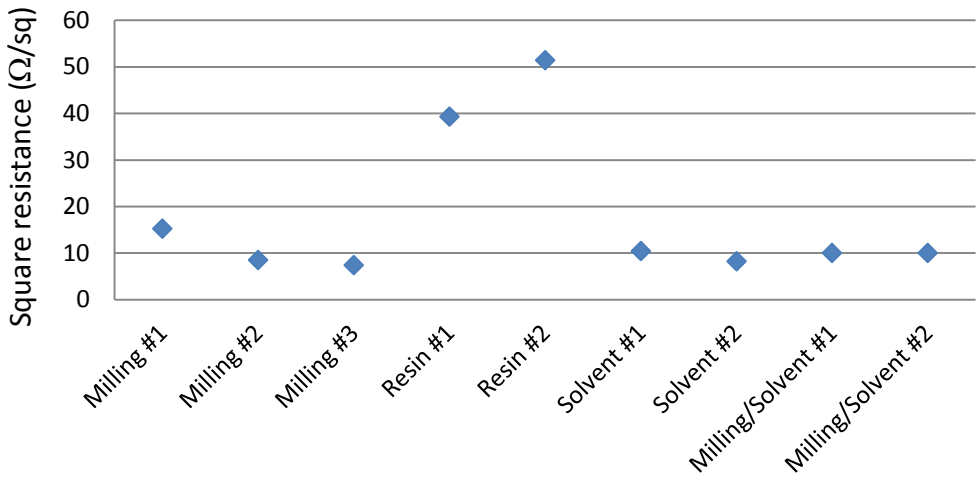

Figure 10: Square resistance (standardized to a layer thickness of 25 µm) of nine different graphene inks. The number of milling passes, the amount of resin and the concentration of the solvent were varied.

Interdigital structures with different dimensions for the electrode fingers and the distances between adjacent fingers were designed and realized on two printing cylinders. The printing cylinders differed in the well depth and the number of lines per cm. It turned out that each of the two printing cylinders was only suitable for printing certain electrode structures (Figure 11). The interdigital structures, which were used by the project partner cellasys already before project start, have dimensions of 50 µm finger width and spacing each. Experiments showed, however, that already electrodes with dimensions of 100 µm finger width and spacing each have the same sensitivity (within the limits of the measuring accuracy). For reasons of lower requirements with respect to the printing process, it was therefore decided to use electrodes with finger dimensions of 100 µm finger width and spacing for the biological experiments and to use a cylinder with a well depth of 50 µm at 80 lines per cm for printing.

To obtain a good printing result, it was necessary to study the influence of printing parameters, such as doctor blade pressure, cylinder contact pressure, printing speed and NIR dryer performance, to finally determine the ideal printing parameters. For the printing of the structures from graphene in the gravure printing method, the following printing parameters proved to be optimal:

- Printing speed: 40 m/min
- Power for corona activation of the film: 600 W

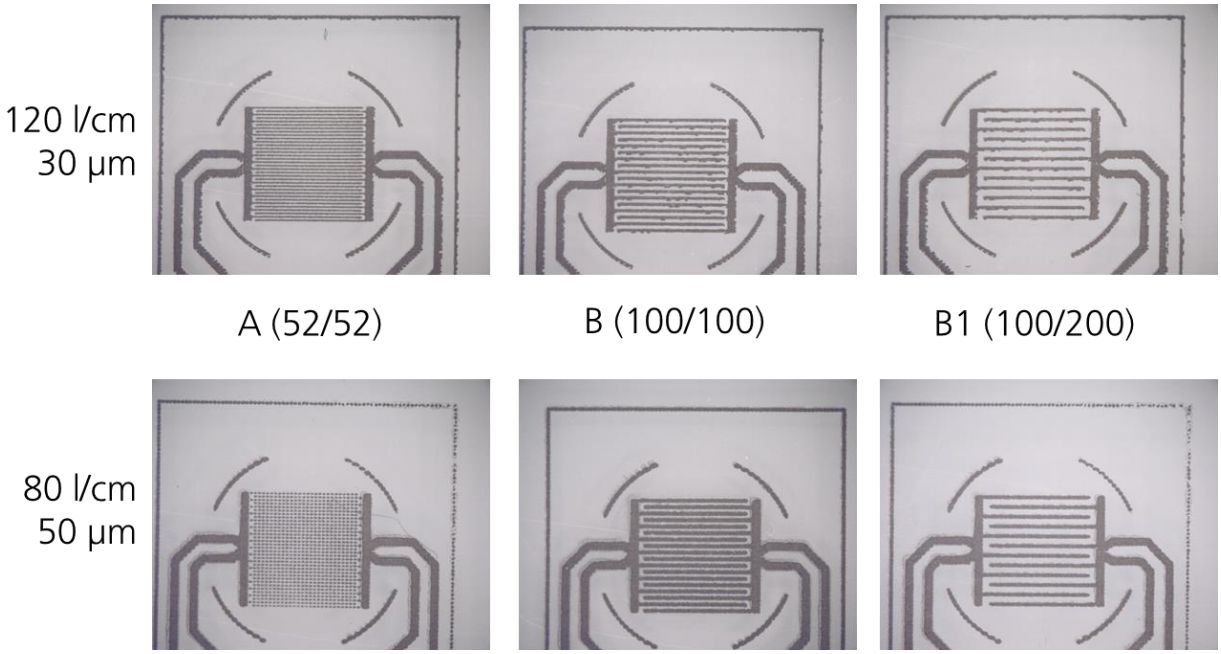

Figure 11: Printed interdigital graphene structures. The printing cylinder for the prints of the upper row had a well depth of 30 µm at 120 lines per cm. The printing cylinder for the prints of the lower row had a well depth of 50 µm at 80 lines per cm. The electrode fingers had different values for finger width and distance between electrode fingers on the photos of the three columns (values in brackets are in the unit µm).

The results concerning printing of graphene electrodes were presented at LOPEC 2018 Conference [14].

Figure 12 shows the photograph of a printed array of interdigital structures arranged in the format of a 96-well plate, using only the positions of every second well. This results in a number of 24 interdigital structures.

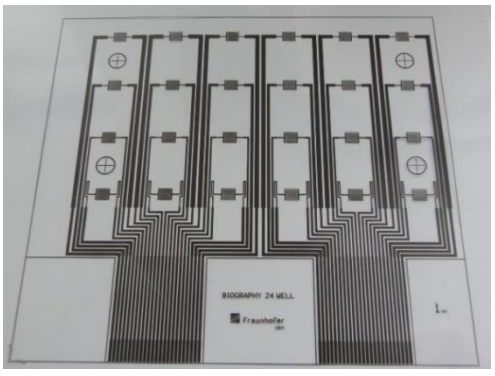

Figure 12: Photograph of a printed array of 24 interdigital structures arranged in the format of a 96-well plate.

The design of the leads to the electrodes is chosen so that theoretically the same resistance value should result for all supply lines. In fact, the values of the printed leads varied from electrode to electrode and ranged from about 10 to 15 kOhm.

3.4.2 Protein coating of graphene electrodes

For initial print tests with a protein ink, a test cylinder manufactured by SAUERESSIG was used. It had structures in the form of circular depressions. The idea behind this was to print the proteins in the form of small dots, which, in spite of a low use of protein material, have a comparable influence on the adhesion behaviour of cells as a continuous protein layer. The test cylinder had circles with depths of 7, 9 and 11 µm and diameters of 5, 10, 20 and 50 µm, respectively. In print trials with this printing cylinder, both the already existing protein base ink of the IBMT and commercial gravure inks were used as print media. A good print image could be achieved only for the circles with a diameter of 50 µm and a depth of 11 µm. These dimensions are almost in the range of the electrode widths. Therefore, the design of the protein structures was changed to print a closed protein layer over the entire area of an interdigitated electrode structure (Figure 13).

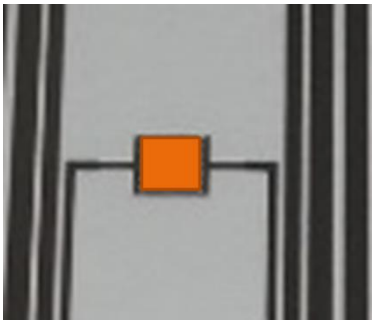

Figure 13: Schematic representation of the protein layer (shown in orange) on an interdigital electrode structure. Graphene conducting paths are black in colour. The interdigital structure lies underneath the orange protein structure.

A protein ink was developed based on the base ink of the IBMT and the addition of Matrigel (dissolved in DMEM/F12). To increase the viscosity, sodium salt of carboxymethylcellulose (dissolved in deionized water) was also added. For gravure printing, the following print parameters proved to be optimal:

- Printing speed: 40 m/min
- Power for corona activation of the film: 600 W

Printing tests showed that the developed protein ink could be printed on the bare PET film and on previously printed graphene patterns.

3.4.3 Two-colour gravure printing

The current two-colour printing system has two printing units that allow the printing of the graphene structure and the subsequent printing of the protein structure in one print run. Graphene and protein patterns were successfully printed in one run using the printing parameters for graphene and protein printing given above. Different approaches for an automatic adjustment of the two prints to each other were tested. Sensors were implemented in the printing system but it turned out that the sensors were too sensitive. As alternative a stroboscope lamp is used. The frequency of the stroboscope is adjusted to the printing speed. Thus the register marks can be checked optically and the servo drives can be regulated in case of a misfit of the register marks.

This readjustment of the protein cylinder in the printing direction leads to an increase or decrease in the web tension. Because of technical problems during the final assembly of the printing machine the web tension control had to be locked in position. If the web tension is not perfect it results in a movement of the web perpendicular to the printing direction. Therefore, the accuracy of the register in printing direction is not high enough up to now.

To circumvent this problem, in addition to the two-colour printing process, a process for the manual coating of graphene structures with Matrigel was developed. The obtained layers of Matrigel had a thickness of about 5 µm. Experiments with manually applied layers of Matrigel showed that the influence the coating had on the electrode impedance measured in a nutrient solution was negligible.

3.5 Evaluation of surface functionalised foils for sensor applications

Printed sensors in multiwell plate format were bonded to bottomless well plates (Figure 14 left). For this purpose, a double-sided adhesive film (Adhesives Research AR 90106) was first glued to the bottomless well plate. The adhesive film was mechanically removed from the wells, which were later to be used for cultivation. Subsequently, the sensor film was bonded to the adhesive film so that the film with the electrodes formed the bottom of the well plate. The connection of the printed contact pads to a board was realized using ZIF (Zero Insertion Force) connectors (Figure 14, right and Figure 15).

Figure 14: Left: Bottomless 96-well plate. Right: Printed polymer film glued to a bottomless 96-well plate. ZIF plugs are added for electrical connection.

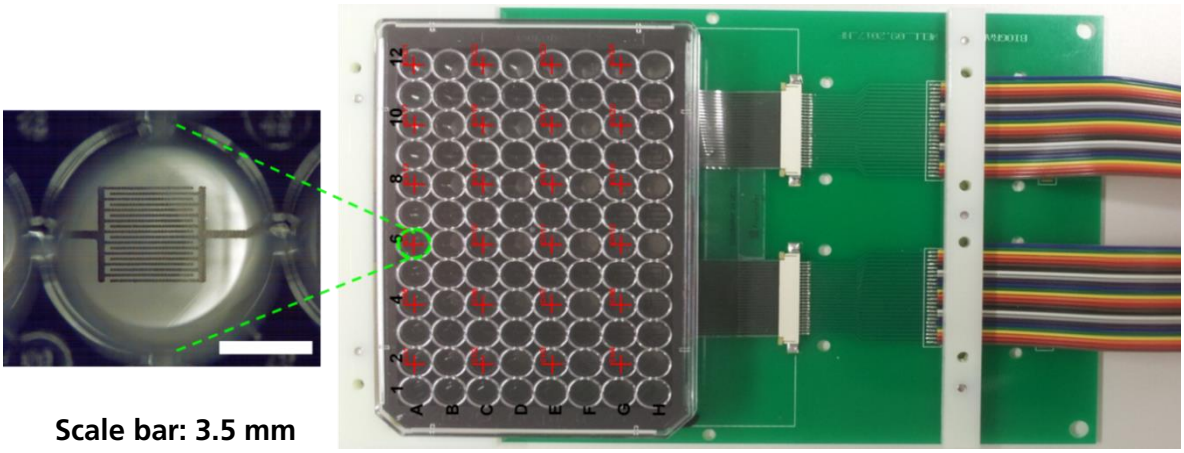

Figure 15: The printed polymer film, glued to a bottomless 96-well plate and with attached ZIF connectors, is connected to a circuit board. The ribbon cables lead to the measuring device. The red crosses indicate the wells with interdigital structures. On the left an enlarged picture of one well with an interdigital structure is shown.

In preliminary experiments, the influence of the growing cells on the impedance values was examined in two plates with 24 wells until the cells were confluent. It turned out that the graphene conductor paths leading to the interdigital structures had high fluctuations in the measured impedance due to their high electrical resistance (10 to 15 kΩ for each of the two finger structures of an interdigital electrode). The variations of about ± 100 Ω for successively measured values were similar to the actual sensor signal, which is the change in impedance caused by the confluent cells.

As a countermeasure, a modified design of the printing cylinder was developed, which, at the expense of the number of usable wells, leads to a lower lead resistance. The lead resistance achieved was 4 to 6 kΩ. However, the above-mentioned fluctuations of the measured impedance values could not be significantly reduced.

In addition, a metal mask was designed and fabricated to sputter-coat previously printed graphene structures in the area of the tracks with a thin metal layer (Figure 16).

Figure 16: Printed sensors with graphene electrodes in the wells and conducting paths coated with gold outside the wells to increase electrical conductivity.

The structure of the gold layer corresponds to the design of the above-mentioned modified printing cylinder. This variant simulates a structure which can be produced purely by printing technology, in which the regions of the supply lines lying outside the wells consist of printed metal structures. For example, silver inks are commercially available, resulting in structures with low electrical resistance, but are not biocompatible and therefore not suitable for cell-contacting interdigital electrodes.

3.5.1 Set-up of printed impedance sensors for validation of antiviral substances

First tests should show that the impedance value increases when cells grow in a well up to confluency. After addition of SDS (sodium dodecyl sulfate), the cells dissolve and the measured impedance should abruptly decrease. Twelve wells were used for this experiment: 6 wells with 1×10^4 cells (TZM-bl) per well and 6 wells without cells. SDS was added to 4 wells each of these two groups after the cells had grown confluently.

The protocol was as follows:

- Time 0 min: Addition of culture medium (all 12 wells)
- Time 1470 min (about 24 h): Removal of medium; addition of new medium (6 wells) and addition of medium with 1×10^4 cells (6 wells)
- Time 5726 min (approximately 96 h): Addition of SDS (in 4 wells with cells and 4 wells with medium).

The measured impedance curves of the individual wells are shown in Figure 17.

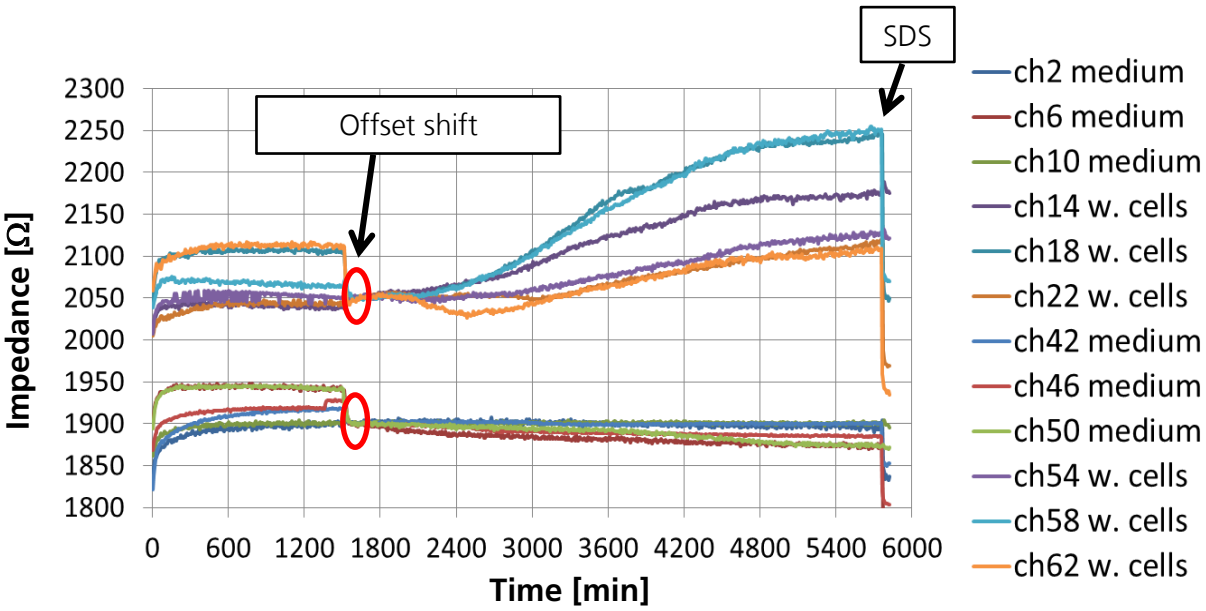

Figure 17: Measurement curves of the preliminary experiment (6 wells with cells, 6 wells filled with medium only). All curves related to wells with cells (upper curves) and all curves related to wells without cells (lower curves) are combined by an offset shift of the measurement curves (see red marking in the diagram). The impedance measurements were obtained at an AC frequency of 10 kHz.

By means of an offset shift of the measurement curves at time 1620 min (27 h), all the curves of the wells with cells as well as all the curves of the wells without cells are combined in each case. It can be clearly seen that in wells with cells (upper curves) the impedance values increase over time, which indicates an electrical insulation of the electrodes by the confluently growing cells. In wells without cells (lower curves), this behaviour cannot be observed. The effect of adding SDS is not readily apparent due to the partially superimposed curves. Therefore, the time range of 5580 to 5880 min (93 to 98 h) is shown enlarged in Figure 18.

In wells without cells, the addition of SDS leads to an impedance change of about 80 ohms. This value must be subtracted from the impedance values of the wells with cells. The average remaining impedance change, which is caused only by the detachment of the cells, is about 100 Ω.

In summary, it was shown that the measured impedance changes when cells cover the electrodes and when the cells are detached from the electrodes. The confluently grown cells as well as the detachment of the cells after addition of SDS could be confirmed by microscopic observations.

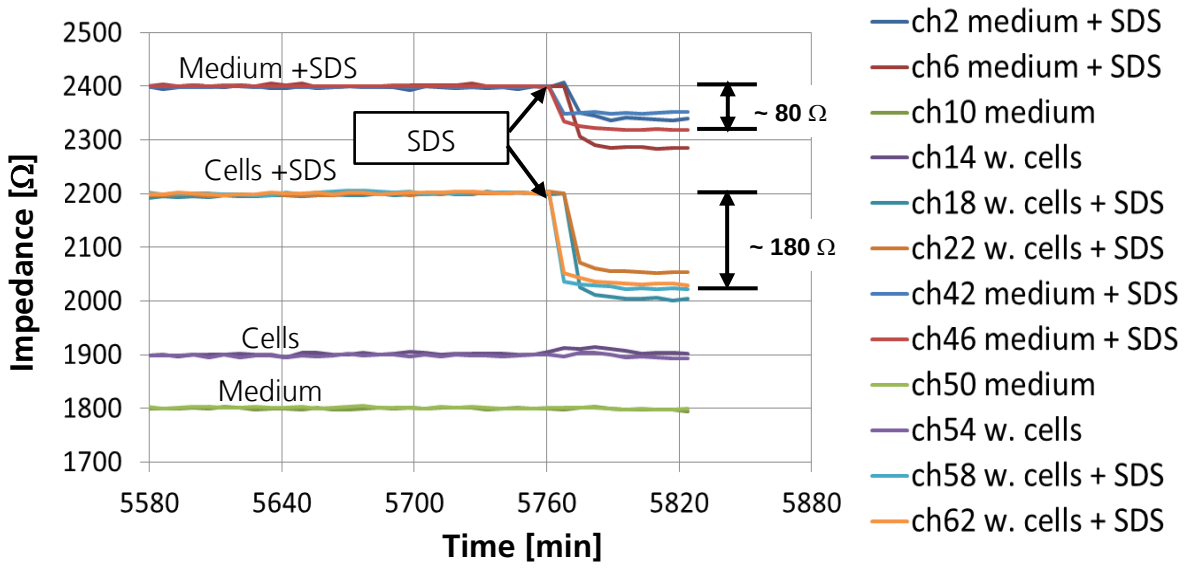

Figure 18: Enlarged representation of the time range from 5580 to 5880 min from Figure 17.

3.5.2 Virus-induced cytopathic effect and its inhibition

In the following it was examined whether impedance curves reflect the virus-induced cytopathic effect on the cell culture and its inhibition by the antiviral substance Efavirenz (non-nucleoside reverse transcriptase inhibitor). To prove this, the TZM-bl / HIV-1 pseudovirus system, which is well established at IBMT, was used.

For this experiment, 12 wells were used:

- 3 wells without cells
- 3 wells with $1x10^4$ cells (TZM-bl) per well
- 3 wells with $1x10^4$ cells (TZM-bl) per well and addition of HIV-1 pseudovirus PVO.4 (1:10 diluted) after 24 h
- 3 wells with $1x10^4$ cells (TZM-bl) per well and addition of HIV-1 pseudovirus PVO.4 (1:10 diluted) plus 1 µl Efavirenz after 24 h

The protocol was as follows:

- Start: Add culture medium (all 12 wells)
- After 4 days: Removal of medium; addition of new medium or addition of medium with $1x10^4$ cells
- After 24 h: Addition of virus stock or virus stock plus Efavirenz

For all 12 wells, the same amount of medium was removed at the time of cell addition and supplemented with new medium. Except for the media control, the newly added medium contained TZM-bl cells. Also with the addition of HIV-1 pseudo virus stock PVO.4 and virus stock plus Efavirenz, the same amount of the same liquid (with / without virus / Efavirenz) was added to all 12 wells. Therefore, short-term impedance changes at the time of fluid addition can be seen in the impedance curves of all 12 wells. The measured impedance curves of the individual wells are shown in Figure 19. In the media controls, the impedance does not change during the measurement. For wells with cells without addition of virus, the impedance values increase continuously as the cells grow to a confluent cell monolayer. The addition of the HIV-1 pseudo virus

stock plus Efavirenz shows a similar behaviour, since the antiviral substance largely inhibits the cytopathic effect. When the viral stock is added alone (bottom curves in Figure 19) a significant viral effect on the cell culture can be seen in the impedance curve. In the time range 2000 to 2500 min (approximately 33 to 42 h), the impedance increases with a constant slope. In the time range 2500 to 3000 min (approximately 42 to 50 h) the slope of the impedance curve changes from positive to negative values. In the time range 3000 to 3500 min (50 to 58 h), the impedance drops at a constant slope.

The change in the slope of the impedance curve can be used as a measure for the extent of the cytopathic effect. An expression of the cytopathic effect normalized to the starting slope of the impedance curve should be defined as follows for the measured values shown in Figure 19:

$$Cytop.\ Effect = \frac{\mathrm{Slope}_{2000\ \mathrm{to}\ 2500\ \mathrm{min}} - \mathrm{Slope}_{3000\ \mathrm{to}\ 3500\ \mathrm{min}}}{\mathrm{Slope}_{2000\ \mathrm{to}\ 2500\ \mathrm{min}}}$$

The values calculated from the curves shown in Figure 19 are shown in Figure 20. There are no meaningful values for the media control, since zero is divided by zero. Figure 21 shows the microscopic assessment of the cells 48 hours after virus addition. Without the addition of the virus stock, the cells have reached a confluency of about 80-90%. For the sample of TZM-bl cells plus PVO.4, the achieved confluence is only 40-50%. With the addition of the pseudo virus stock plus Efavirenz, the cells reach a confluence of about 80%.

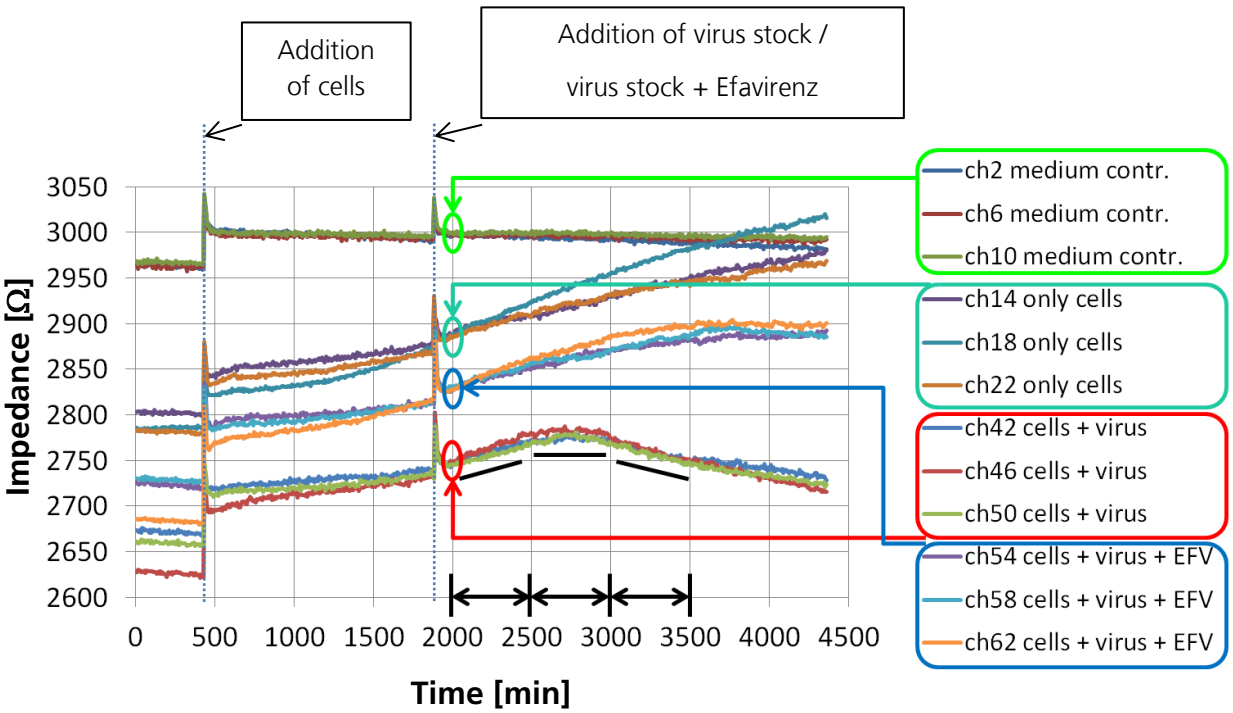

Figure 19: Measurement curves of all 12 wells. The legend indicates whether medium or cells were in the respective wells and whether only HIV-1 pseudo virus stock PVO.4 or PVO.4 plus Efavirenz was added. By means of an offset shift of the measured curves, all curves of a group are combined. From the first 4 days of incubation without cells, only the last 400 min are shown.

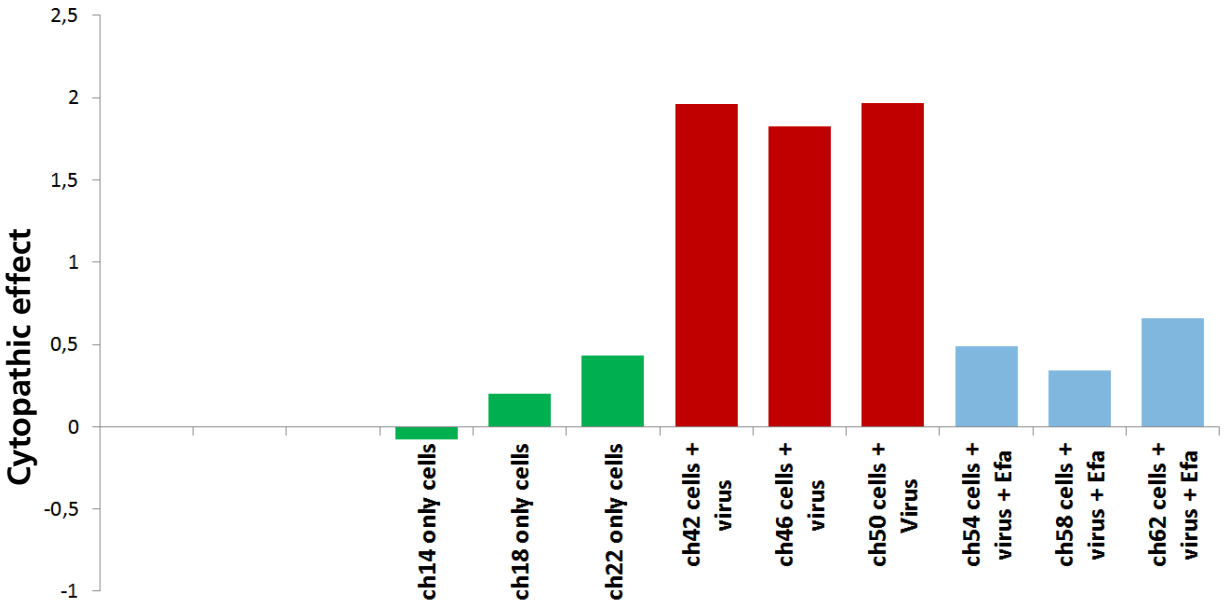

Figure 20: Strength of cytopathic effect calculated with the values from Figure 19 according to the formula given above. For the media control, the calculation does not make sense.

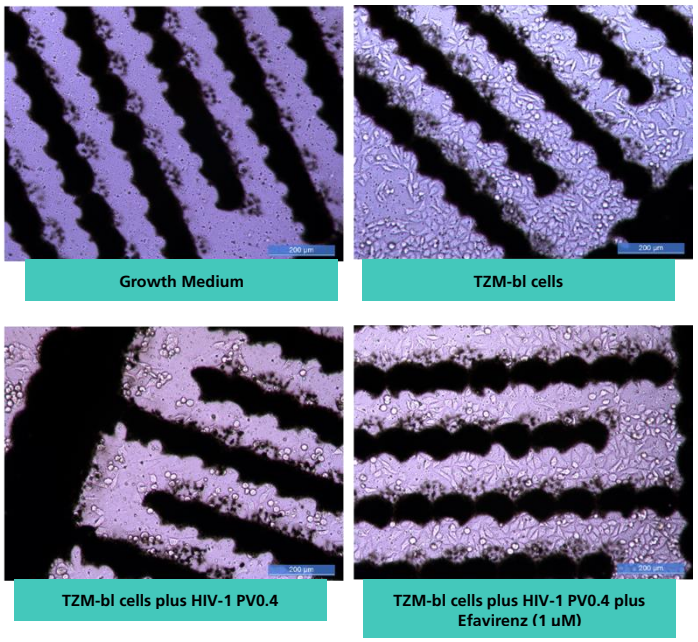

Figure 21: Microscopic evaluation of the wells 48 hours after infection of the TZM-bl cells with the HIV-1 pseudo virus PVO.4. The black areas correspond to the electrodes made of graphene. Only the areas between the electrodes can be observed microscopically. Top left: Wells with medium show no cells. Upper right: TZM-bl cells of the cell control have reached 80-90% confluence. Bottom left: 40-50% confluence after virus infection of TZM-bl cells. Bottom right: In the presence of the antiviral substance Efavirenz, 48 h after infection with the virus stock PVO.4, the cells show a confluence of about 80%. Blue scale bars: 200 µm.

3.5.3 Cytopathic effect at different virus concentrations

The expression of the cytopathic effect on the cell culture depends on the virus concentration. In order to check whether this is reflected in the impedance curves, a further series of experiments was carried out. The pseudo virus stock PVO.4 was added in four different concentrations (5-fold dilution series). For this experiment, 12 wells were used:

- 2 wells without cells
- 2 wells with 1 x 10^4 cells (TZM-bl) per well
- 4 wells with 1 × 10^4 cells (TZM-bl) per well and addition of HIV-1 pseudo virus PVO.4 (1:10, 1:50, 1: 250, 1: 1250) after 24 h
- 4 wells with 1 x 10^4 cells (TZM-bl) per well and addition of HIV-1 pseudo virus PVO.4 (1:10, 1:50, 1: 250, 1: 1250) plus 2 µM Efavirenz after 24 h

The process was as follows:

- Start: Add culture medium (all 12 wells)
- After 24 hours: Removal of medium; addition of new medium or addition of medium with 1 x 10^4 cells
- After another 24 hours: Infection of the TZM-bl cells with the HIV-1 pseudo virus PVO.4 or PVO.4 plus Efavirenz

The measured impedance curves of the individual wells are shown in Figure 22.

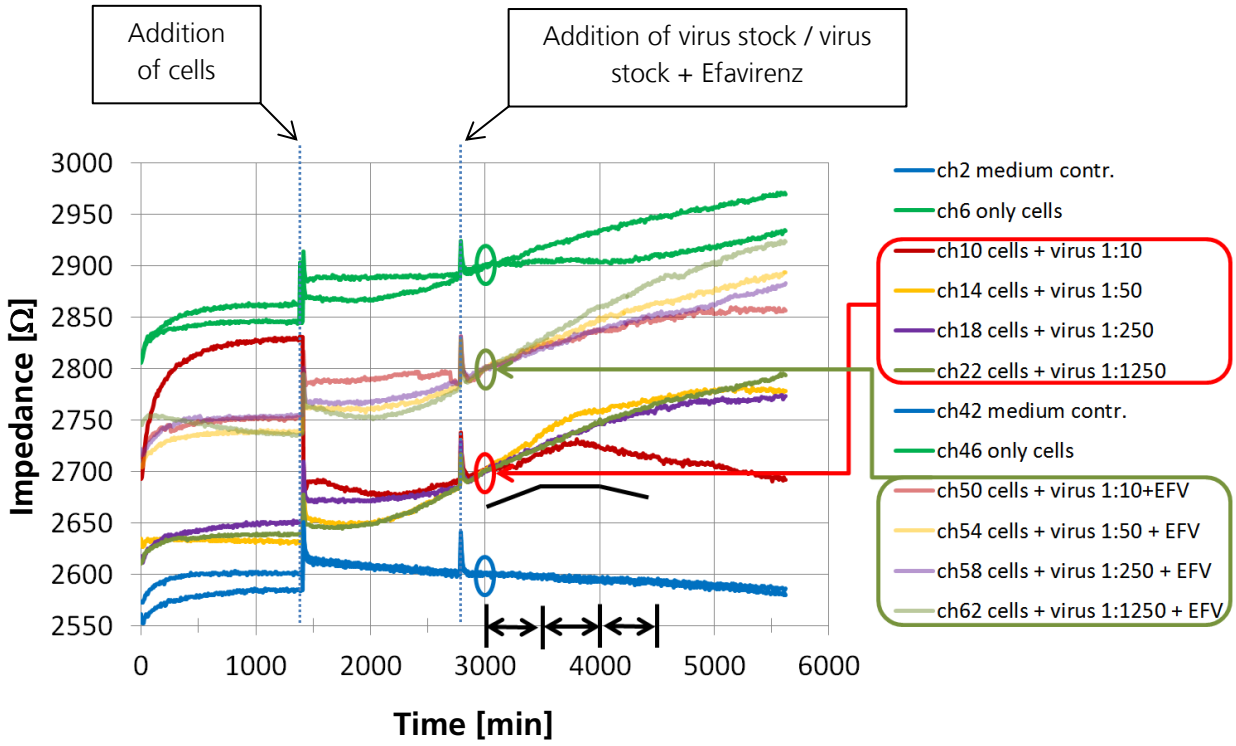

Figure 22: Curves of all 12 wells. By means of an offset shift of the measured curves, all curves of a group are combined.

The change in the slope of the impedance curve should again be used as a measure for the ex-

tent of the cytopathic effect and is calculated according to the formula given above. Since the turning point of the curve with the strongest cytopathic effect (curve "ch10 cells + virus 1:10") lies at a different time compared to Figure 19, the formula should be modified as follows:

$$Cytop.\ Effect = \frac{\text{Slope}_{3000 \text{ to } 3500 \text{ min}} - \text{Slope}_{4000 \text{ to } 4500 \text{ min}}}{\text{Slope}_{3000 \text{ to } 3500 \text{ min}}}$$

The calculated values are shown in Figure 23. It can be clearly seen that the expression of the cytopathic effect increases with increasing virus concentration and this can be observed in the impedance curve. In the presence of the non-nucleoside reverse transcriptase inhibitor Efavirenz, the inhibition of the viral infection can be detected by a reduction in the CPE, with the impedance signal almost at the level of the cell control (ch46).

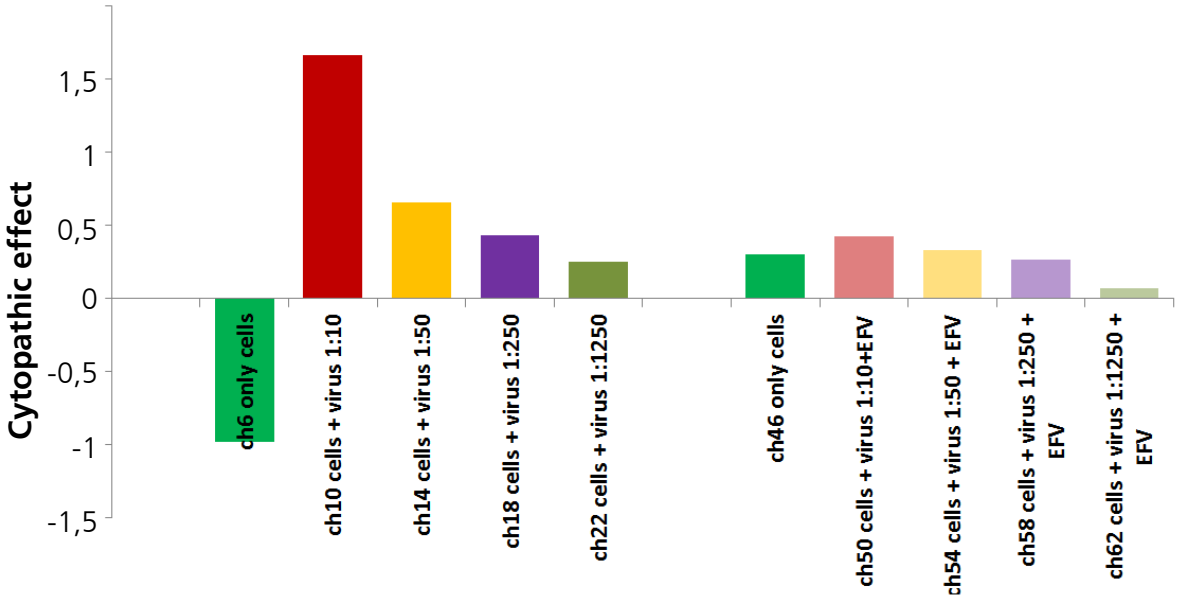

Figure 23: Strength of the cytopathic effect calculated from the values of Figure 22 according to the formula given above. For the media control, the calculation does not make sense.

The following figures (Figure 24, Figure 25) show the microscopic evaluations of the cells 48 hours after addition of the different virus concentrations (Figure 24) or the addition of different virus concentrations together with Efavirenz (Figure 25). In cell control without addition of the HIV-1 pseudo virus stock PVO.4, the cells reached approximately 80-90% confluence. When PVO.4 is added, the achieved confluency depends on the virus concentration. As expected, the lower the virus concentration, the greater the confluence. The microscopically determined values of confluence match very well with the measured impedance curves and the calculated values for the expression of the cytopathic effect.

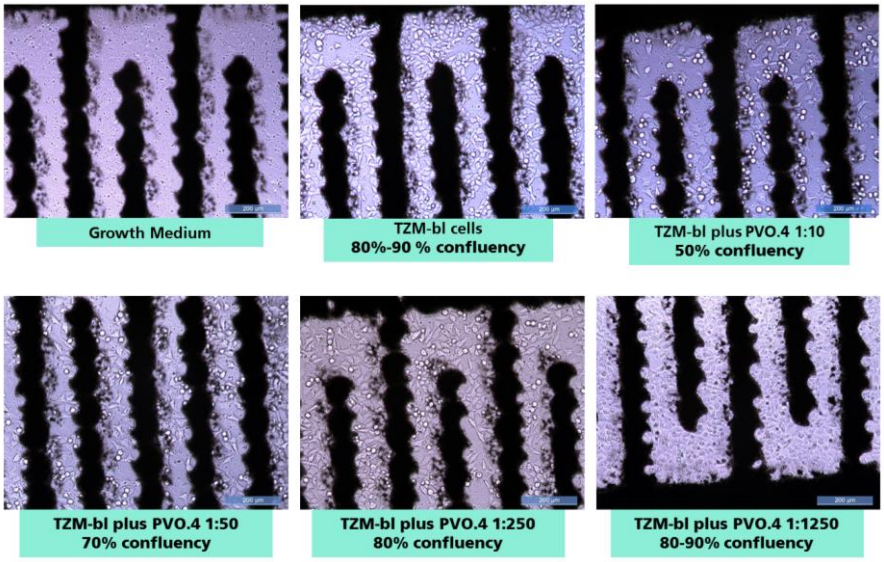

Figure 24: Microscopic assessment of TZM-bl cells 48 hours after virus addition. The black areas are the graphene electrodes. Only the areas between the electrodes can be observed microscopically. The visually determined confluence values are indicated in the green text fields. Blue scale bars: 200 µm.

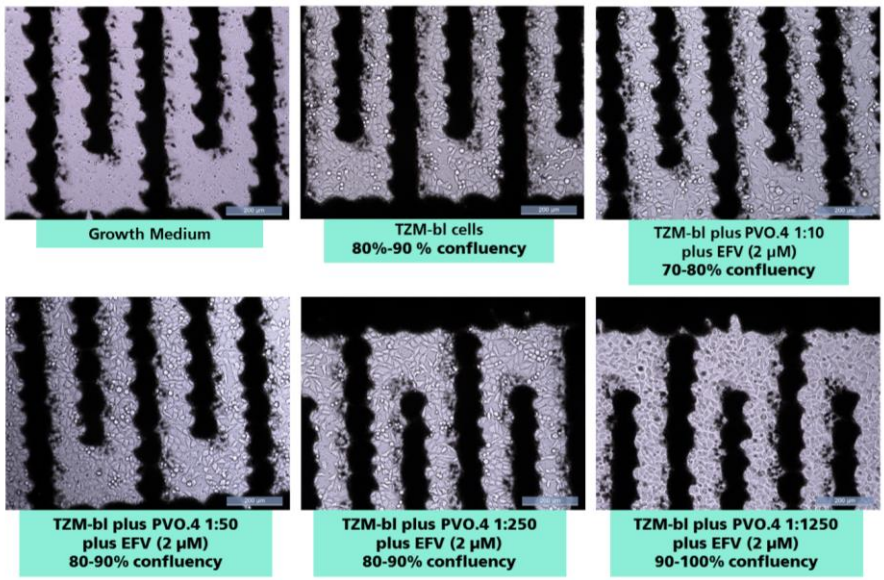

Figure 25: Microscopic evaluation of the cells 48 hours after addition of virus plus Efavirenz. The black areas are the graphene electrodes. Only the areas between the electrodes can be observed microscopically. The visually determined confluence values are indicated in the green text fields. Blue scale bars: 200 µm.

3.5.4 Cytopathic effect depending on infectivity of viruses

A well-known phenomenon in the generation of HIV-1 pseudovirus stocks in cell culture-based systems is the occurrence of different infectivity, which are, among others, virus-type specific. The classification of HIV-1 pseudovirus viruses with low, medium and high infectivity was based on the results of the luciferase assay, which is given as a dilution of a virus stock to achieve a RLU (relative luminescence unit) of 150,000.

According to this definition, the viruses to be used in the luciferase assay are as follows:

- "low titer" viruses: undiluted to <1:10,
- "middle titer" viruses: > 1:10 and <1:50,
- "high titer" viruses: > 1:50.

We tested whether this distinction is possible with measured impedance curves. To this end, the virus stock PVO.4, which was characterized with a high infectivity (1:90 dilution at an RLU of 150,000), was pre-diluted with medium in order to get a virus with medium (1:45 or 1:22 with a RLU of 150,000) and low infectivity (1:9 with a RLU of 150,000).

In the impedance measurement experiment, these dilutions correspond to the different virus concentrations, with the lowest final dilution 1:10 in the well reflecting the "high titer" virus, the final dilutions 1:20 and 1:40 in the well reflecting the "middle titer" virus and the lowest concentration (1: 100 dilution) in the well reflecting the low titer virus.

To verify the robustness of the measuring plates, this assay setup was performed in duplicate and thus used a total of 12 wells:

- 2 wells without cells
- 2 wells with 1 x 10^4 cells (TZM-bl) per well
- 2 wells with 1 × 10^4 cells (TZM-bl) per well and addition of HIV-1 pseudo virus PVO.4 (final dilution 1:10 after 24 h
- 2 wells with 1 × 10^4 cells (TZM-bl) per well and addition of HIV-1 pseudo virus PVO.4 (final dilution 1:20 after 24 h
- 2 wells with 1 × 10^4 cells (TZM-bl) per well and addition of HIV-1 pseudo virus PVO.4 (final dilution 1:40 after 24 h
- 2 wells with 1 × 10^4 cells (TZM-bl) per well and addition of HIV-1 pseudo virus PVO.4 (final dilution 1:100 after 24 h

The process was as follows:

- Start: Add culture medium (all 12 wells)
- After 96 hours: Removal of medium; addition of new medium or addition of medium with 1 x 10^4 cells
- After another 24 hours: Infection of the TZM-bl cells with the HIV-1 pseudo virus PVO.4 and the different concentrations corresponding to a virus stock with low, medium and high infectivity

The measured impedance curves of the individual wells are shown in Figure 26.

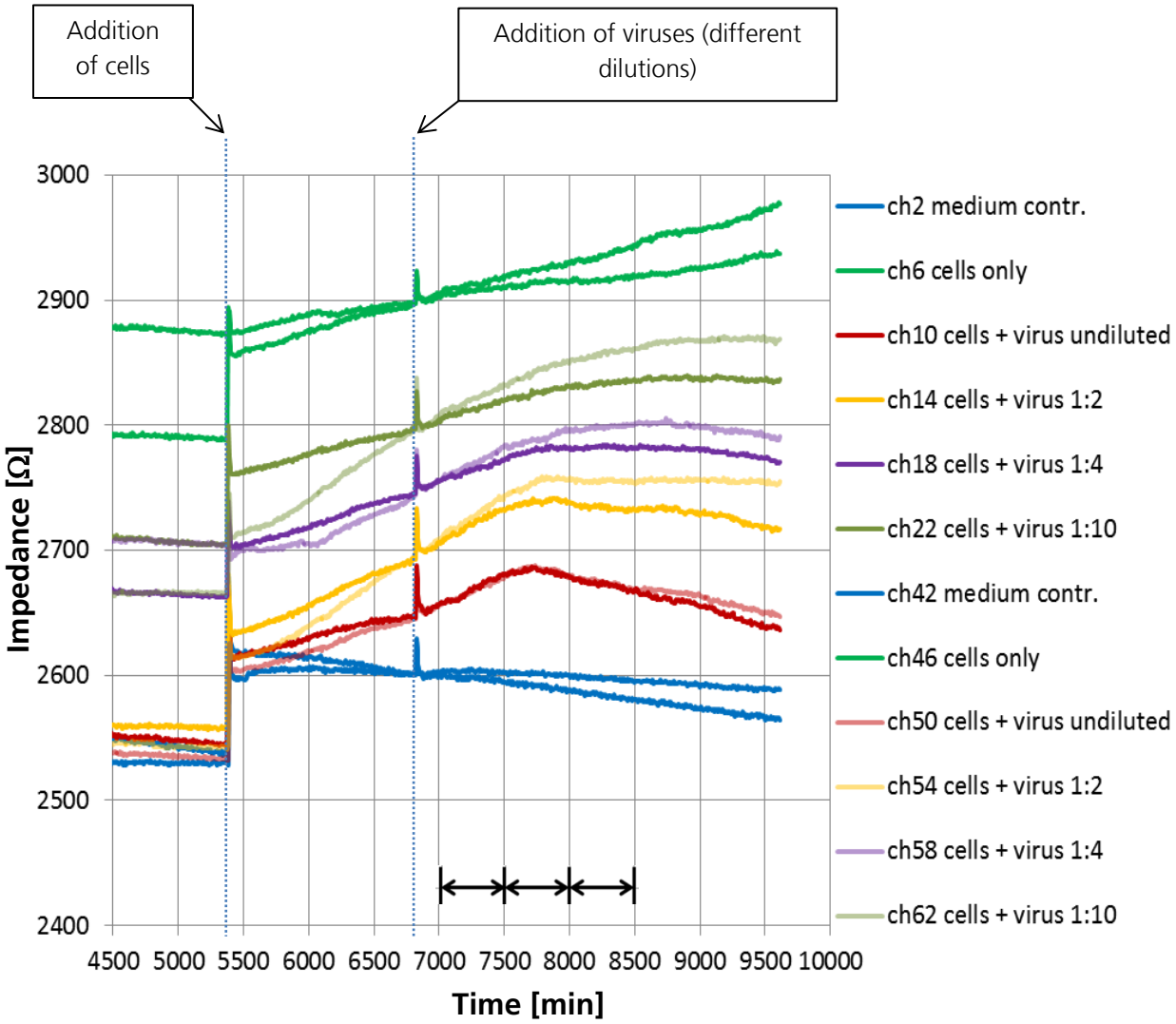

Figure 26: Curves of all 12 wells. By means of an offset shift of the measured curves, pairs of curves belonging to wells with the same content are combined.

The change in the slope of the impedance curve should again be used as a measure for the extent of the cytopathic effect and is calculated like before:

$$Cytop.\ Effect = \frac{\mathrm{Slope}_{7000\ \mathrm{to}\ 7500\ \mathrm{min}} - \mathrm{Slope}_{8000\ \mathrm{to}\ 8500\ \mathrm{min}}}{\mathrm{Slope}_{7000\ \mathrm{to}\ 7500\ \mathrm{min}}}$$

The calculated values are shown in Figure 27. It can be clearly seen that the expression of the cytopathic effect increases with increasing virus concentration, i.e. with infectivity, and that this behaviour is reflected by in the impedance curve.

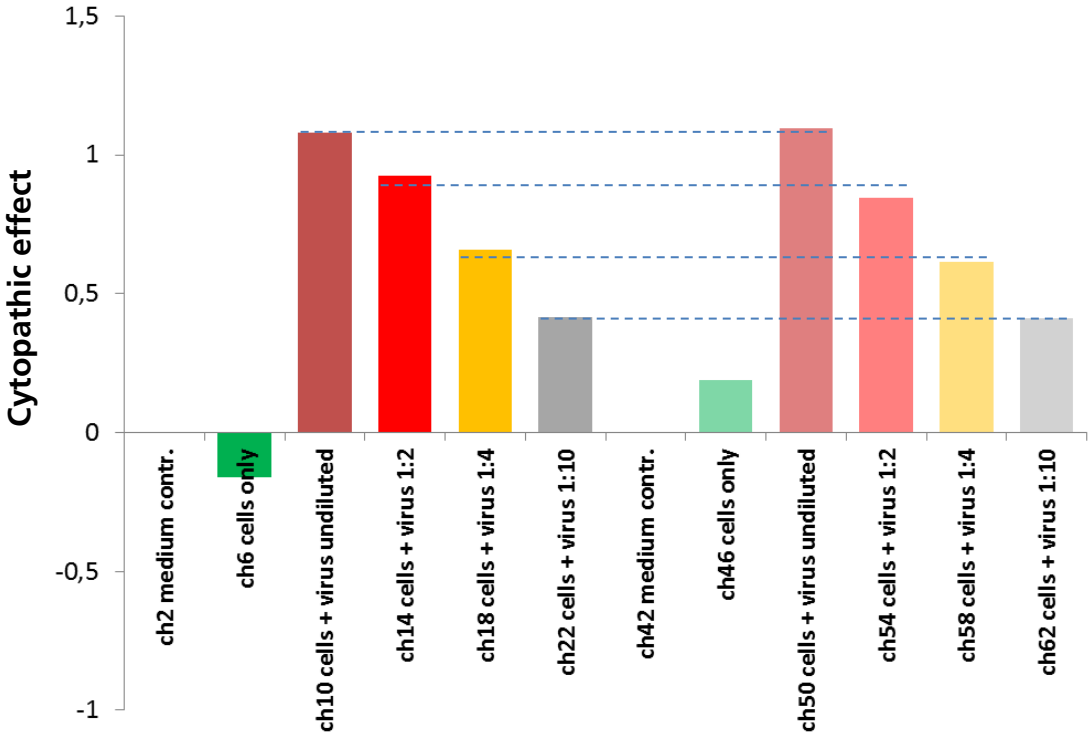

Figure 27: Strength of the cytopathic effect calculated from the values of Figure 26 according to the formula given above. For the media control, the calculation does not make sense. The horizontal dotted lines make clear that the quantitative results achieved for wells with identical virus concentration were almost identical.

Conclusion: In all experiments with cells, the impedance values measured with printed sensors showed the expected behaviour. After cell adhesion, the impedance values increased continuously. When the cells were detached from the surface, the impedance values dropped immediately. The microscope images taken at the end of an experiment showed that the impedance values correspond to the optically determined values for the confluency. In contrast to the optical end point results, the printed impedimetric sensor allows the continuous real-time recording of confluence, and thus the interaction between cells and chemical and biological materials.

3.5.5 Set-up of printed sensors for toxicology

A set-up for long-term monitoring of living cells was provided based on the existing IMOLA-IVD technology of cellasys. To be able to make an electronic contact to the printed sensor a sandwich based contact system as shown in Figure 28 was used.

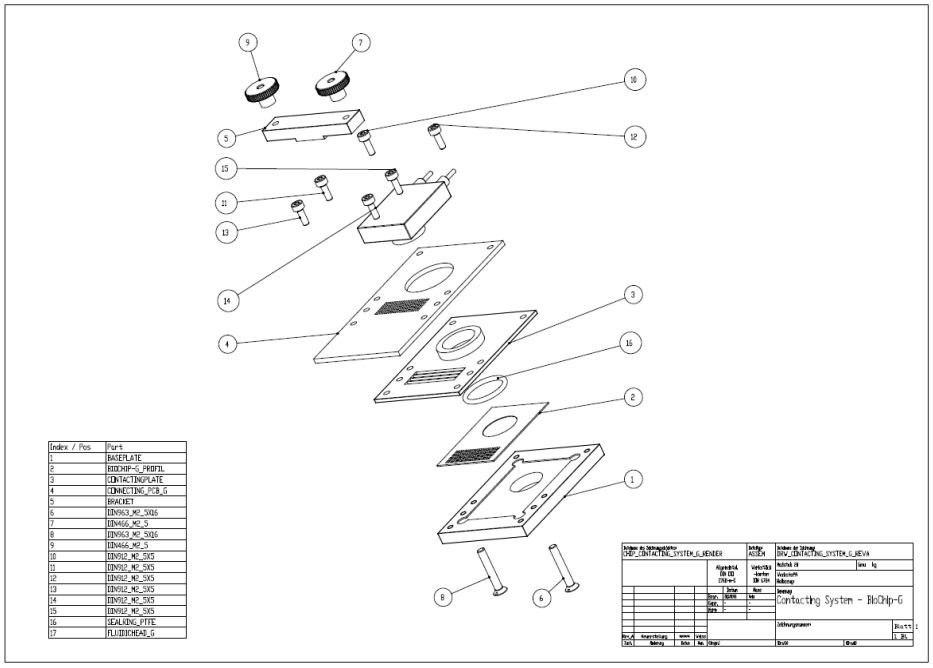

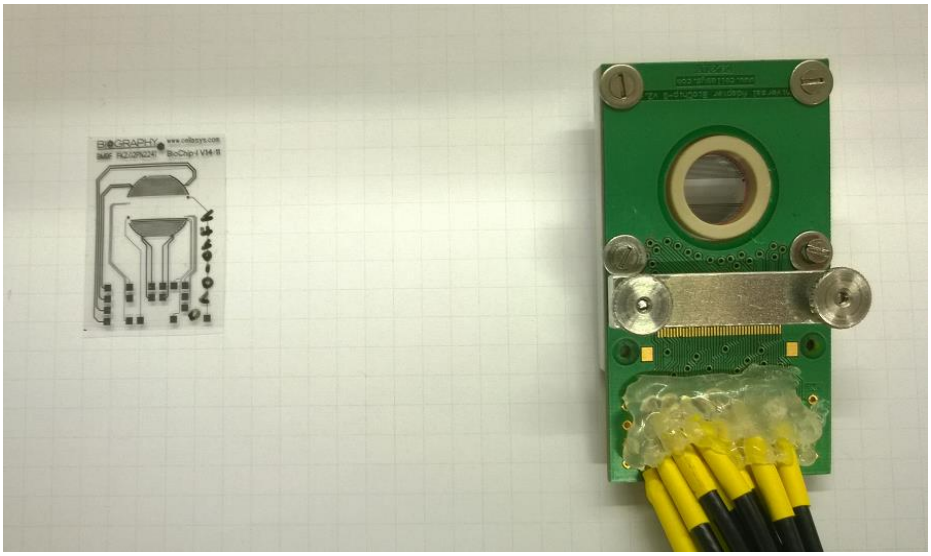

Figure 28: Contact system for the printed sensors with sandwich assembly. Top: Technical drawing. Bottom: Picture of printed sensor and IMOLA adapter.

The contact system was connected to one IMOLA system to read out the impedance values and to supply the cells with cell culture medium. Data were transferred to a PC where cellasys' proprietary DALiA client software collected the data.

3.5.6 Evaluation of printed impedance sensors for validation of antiviral substances

Herpes simplex virus (HSV-1) is reported to produce marked cytopathic effect in different cell lines such as Vero cells from the kidney of *Chlorocebus aethiops* (green monkey). In order to demonstrate a first proof of concept for the analysis of the antiviral effect of test items for antiviral drug discovery by using the printed impedance sensors the impedance of Vero cells infected

with HSV-1 were monitored for 5 days post-infection and compared to non-infected cells, and to infected cells treated with pritelivir, a highly effective antiviral drug. Pritelivir is a thiazolylphenyl derivative and inhibits the helicase–primase complex of herpes viruses [15]. It has been reported that the mean 50% effective concentration (EC_{50}) and the mean EC_{90} values of pritelivir for the SC16 cl-2 strain were 0.01 µM and 0.03 µM, respectively, in cell culture based on cytopathic effect or plaque-reduction assays [16].

The experimental setup was as follows:

- t_1 = 0 min (start of the experiment): Culture medium (DMEM, 10% FCS, L-glutamine) was added to all wells
- t_2 = 1323 min: At day one the medium was replaced by fresh medium or by medium containing 2.5 x 10^4 Vero cells
- t_3 = 2520 min: One day after adding the cells they were infected with HSV-1 SC16 cl-2 in two different infectious doses (50 or 500 infective units/ well). In addition the antiviral drug pritelivir was added in a final concentration of 1 µM (= 100 fold the EC_{50})
- t_4 = 2580 min: After adsorption for one hour the virus was removed by washing with PBS and adding fresh culture medium (DMEM, 1% FCS, L-glutamine) with or without 1 µM pritelivir
- t_5 = 9800 min: End of the experiment at day five post infection

Samples:

Well 1, 7: Culture medium (at t_1)

Well 2, 8: Culture medium (at t_1), Vero cells (at t_2)

Well 3, 9: Culture medium (at t_1), Vero cells (at t_2), HSV-1 SC16 cl-2 in an infectious unit of 50/ well (at t_3)

Well 4, 10: Culture medium (at t_1), Vero cells (at t_2), HSV-1 SC16 cl-2 in an infectious unit of 500/ well (at t_3)

Well 5, 11: Culture medium (at t_1), Vero cells (at t_2), HSV-1 SC16 cl-2 in an infectious unit of 50/ well (at t_3), 1 µM pritelivir (at t_3 and t_4)

Well 6, 12: Culture medium (at t_1), Vero cells (at t_2), HSV-1 SC16 cl-2 in an infectious unit of 500/ well (at t_3), 1 µM pritelivir (at t_3 and t_4)

The impedance curves of the individual wells are shown in Figure 29.

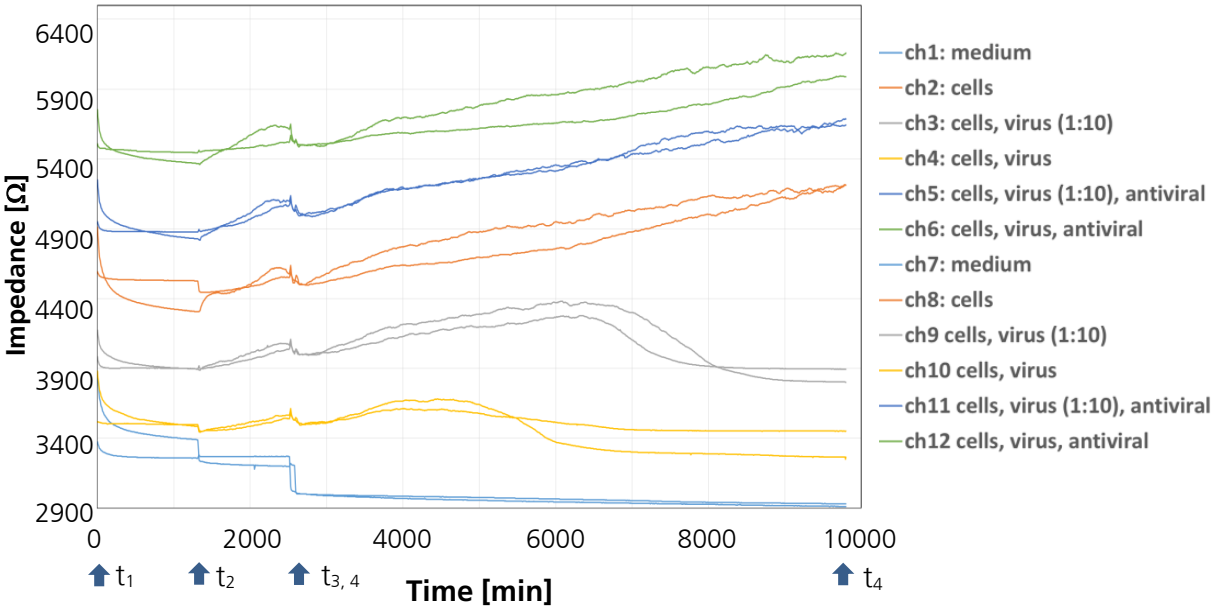

Figure 29: Antiviral activity of pritelivir demonstrated by measuring the impedance over the time of HSV-1 infected Vero cells using the printed impedimetric sensor. By means of an offset shift of the measured curves, pairs of curves belonging to wells with the same content are combined. The legend indicates whether the samples contains medium, uninfected cells, HSV-1 SC16 cl-2 infected cells or pritelivir treated HSV-1 SC16 cl-2 infected cells.

After the end of the impedance measurement 25 µl of PrestoBlue® reagent, a resazurin-based solution that functions as a cell viability indicator by using the reducing power of living cells, was added to each well. After an additional incubation for 1 hour the cell viability was measured. Results are depicted in Figure 30.

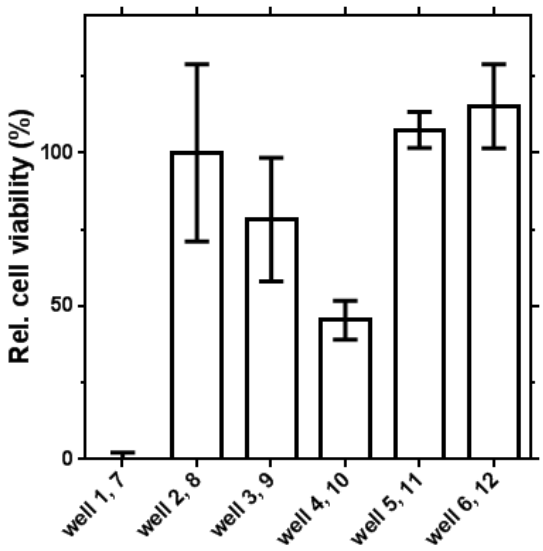

Figure 30: After impedance measurement of HSV-1 infected Vero cells PrestoBlue® reagent was added to each well and the relative cell viability was measured. See the sample/ well description in the text above.

Conclusion:

In the experiment with Vero cells and HSV-1 virus, the impedance values measured with printed sensors showed the expected behaviour. After cell adhesion, the impedance values were increasing continuously, since the cells are more and more covering the electrodes from the surrounding culture medium. After the cells died due to the infection with virus they detached from the surface and the impedance values started decreasing. In contrast to classically used optical endpoint plaque-reduction assays, the printed impedimetric sensor allowed the continuous real-time recording of the cell status. It was therefore possible to detect differences in the killing kinetics for the two different HSV-1 infectious doses used in the experiment. The impedance values of cells infected with the high infectious dose started earlier to decrease than the impedance values of cells infected with the low infectious dose.

To verify that the impedance measurement reflect the cytopathic effect caused by virus infection and to verify that a highly effective antiviral can compensate this effect, the cells from the printed impedance sensor plate were analysed following the end of the experiment with a second method. After adding PrestoBlue® to the cells it could be demonstrated that the reduction in impedance values correlates with a reduction in cell viability caused by virus infection and that cell viability could be restored by treating the cells with an antiviral.

In conclusion, it could be demonstrated that the antiviral activity of a test compound could be proven by measuring the impedance of infected cells treated with the test compound. However, it has to be taken into account, that pritelivir is a highly effective antiviral and was dosed in this proof of concept study in high concentrations of 100-fold the EC_{50}. For this reason further studies with the printed impedimetric sensor have to show whether or not it will be possible to identify the antiviral activities of less potent screening compounds.

3.5.7 Evaluation of printed sensor for toxicology

For evaluation of the printed sensors for a repeated dose experiment a long-term experiment using cellasys technology was designed and implemented. Figure 31 depicts results from a 28 day proof-of principle experiment. The results were published in the ALTEX Proceedings [17] and a book chapter [18].

The printed microstructures were evaluated towards recording of changes in cellular impedance and also for monitoring of extracellular acidification rate. The results showed that impedance monitoring is possible with a similar sensitivity as with conventional biochips. Furthermore a recording of extracellular acidification using the printed microstructures is possible. The following figures (Figure 32, Figure 33) show examples of impedance and extracellular acidification recording with living L929 fibroblast cells.

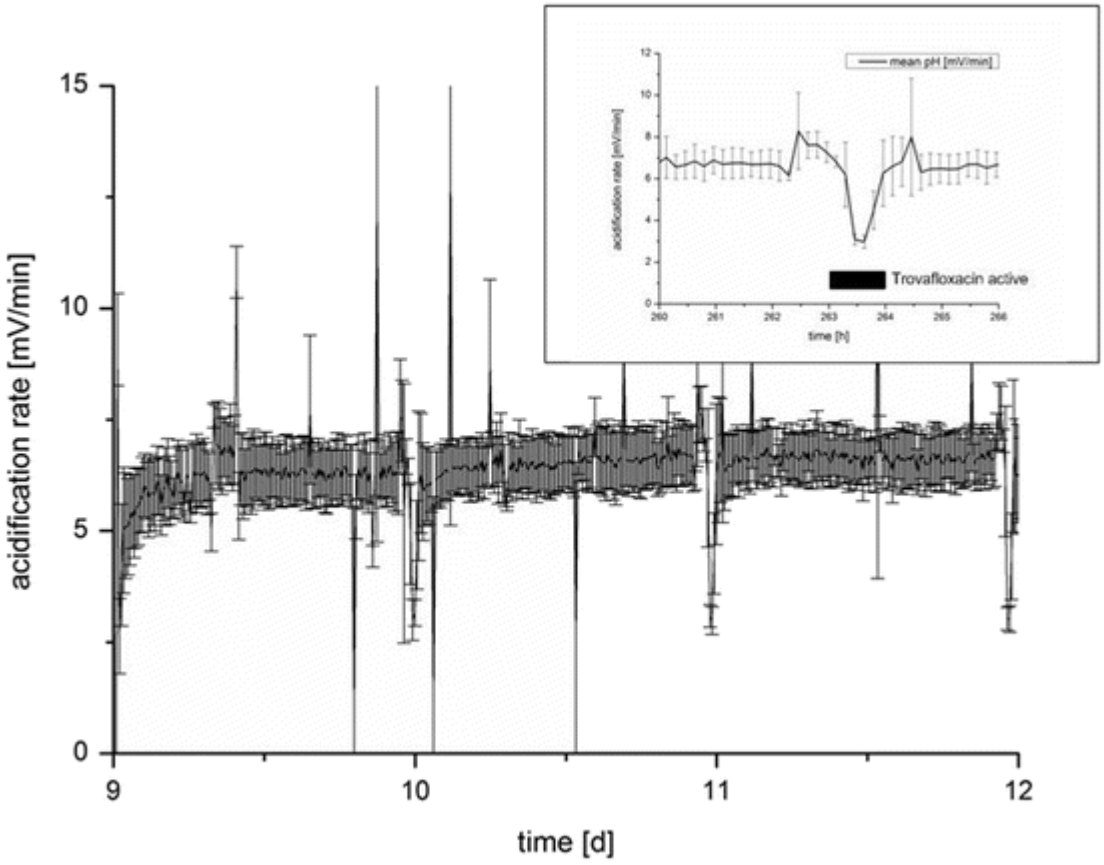

Figure 31: Proof-of-principle experiment of a long-term repeated dose assay. Inset: Zoomed view of reduction of the acidification rate due to the addition of Trovafloxacin at the end of day 11.

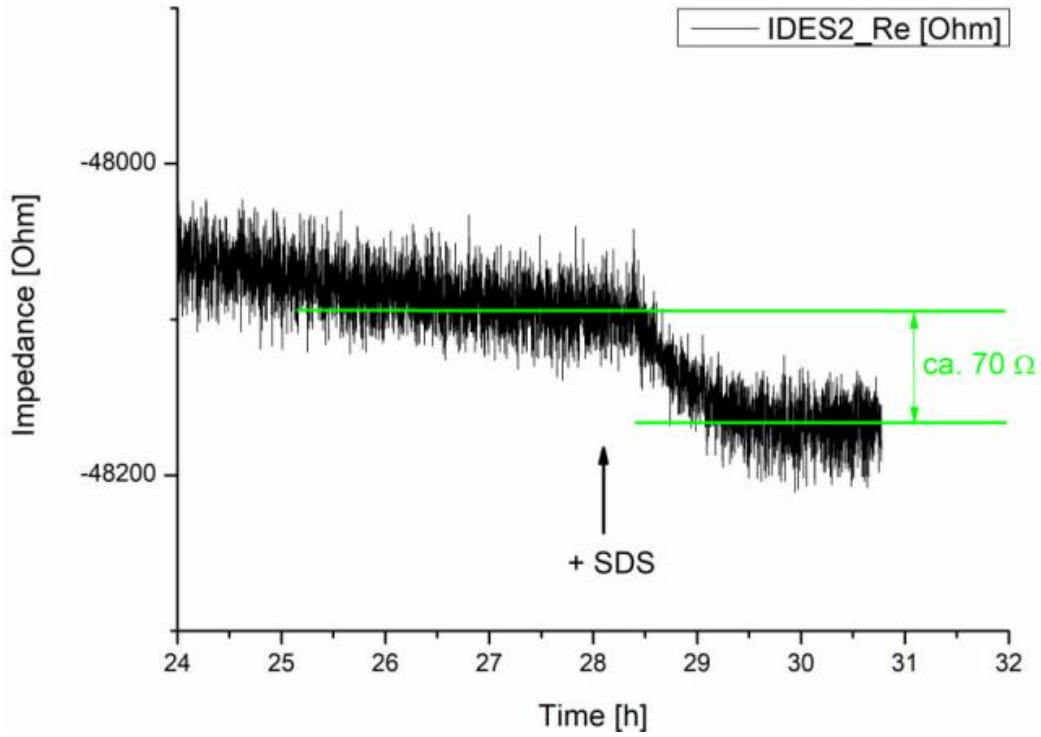

Figure 32: Monitoring of L929 fibroblast cells by means of impedance.

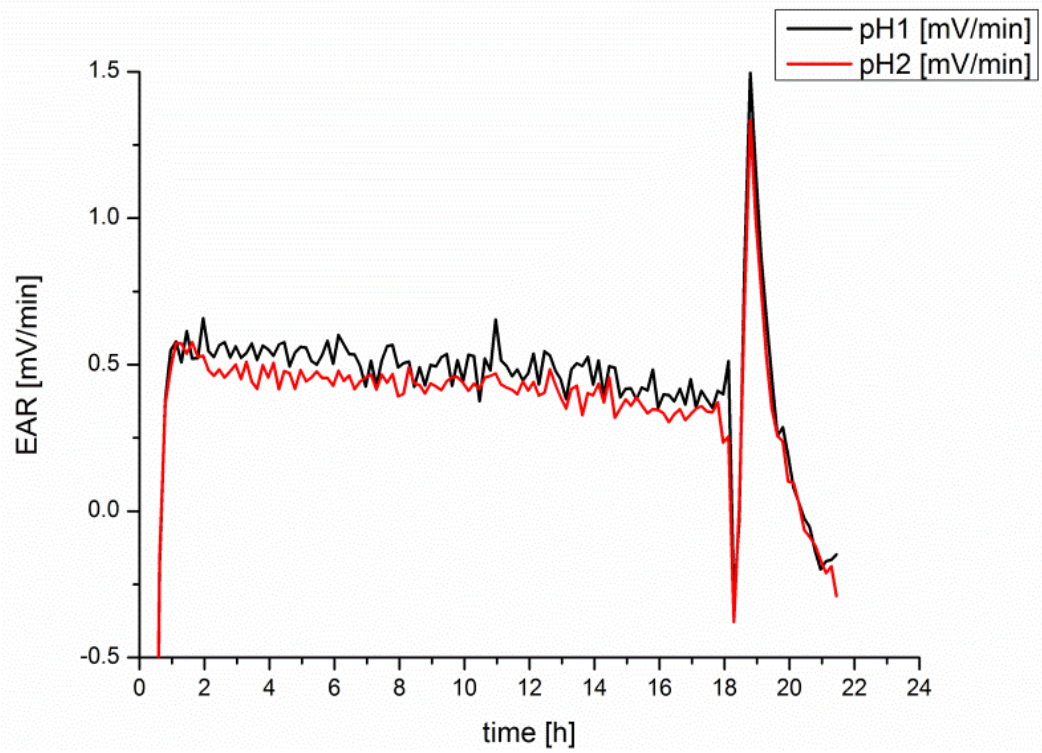

Figure 33: Monitoring of L929 fibroblast cells by means of extracellular acidification rate.

In conclusion the results show that is was possible to evaluate the printed sensor technology successfully for applications in toxicology.

3.6 Production line for roll-to-roll surface functionalization of foils by two-colour-printing

Based on the printed results obtained at Fraunhofer IBMT in the previous work packages as well as on the SAUERESSIG in-house know-how in the field of roll-to-roll production, SAUERESSIG manufactured a production line that is capable of surface functionalization with graphene and proteins in a single roll-to-roll process.

The new production line is based on a one-colour printing machine previously existing at Fraunhofer IBMT (Figure 34). A method for roll-to-roll printing of proteins had been established on this machine. This machine could only be used for printing of one ink at the same time. Thus, printing of well-aligned multilayers was not possible. The available printing machine was the result of a former research collaboration between Fraunhofer IBMT and SAUERESSIG within the project 'BIOREEL'. Further, within the BIOREEL project, Fraunhofer IBMT had developed a biocompatible protein ink as well as processes for printing of protein micro patterns. With these processes it had been demonstrated that cell adhesion can be influenced by printed protein patterns. Thus, multilayers of printed graphene and protein patterns, which partly cover the graphene layer, are expected to lead to electrically conductive electrodes with high affinity for cells. The existing one-colour printing machine had to be adapted and fundamentally expanded. Some parts (e.g. the corona activation) were maintained. Most of the other parts had to be newly designed.

Figure 34: One-colour roll-to-roll printing machine of Fraunhofer IBMT; status before the start of the BIOGRAPHY project.

The design of the two-colour printing machine is in such a manner that also printing with only one printing unit is possible. In case of printing with the first printing unit only, the drying module of the second printing unit can likewise be used if required. Before the polymer film passes the first printing unit it runs through the corona activation unit and thereby the surface energy of the polymer film is increased. Through this activation especially the transfer of aqueous inks from the printing cylinder to the polymer film is highly enhanced. The printing conditions can be controlled precisely by digital gears. Micrometer gears and linear guiding enable an accurate adjustment of the contact pressure or the printing slot. The process parameters can be regulated digitally by a touch panel.

The printing units had to be adapted to the two-colour printing whereas the size of the cylinders with a diameter of 100 mm and a width of 300 mm was not changed compared to the existing one-colour printing machine. A completely new construction of the printing units was made. The printing cylinder can be laterally moved within the printing unit by micrometer screws. Thus the lateral printing position of one printing ink relative to the other – i.e. the lateral register – is controlled manually by these micrometer screws. This is a fail-safe and widespread system. The alignment of the two printing cylinders to each other in printing direction is more complicated. Both printing cylinders possess register marks in the shape of crosses and triangles. A sensor positioned behind the second printing unit measures the exact position of the second register mark relative to the first one. In case of a misfit in the printing direction the servo drives regulate the speed of the printing cylinders so that the printing marks of both cylinders are aligned. To ensure the functionality with several inks different sensors were ordered. After implementation it turned out that the sensors were too sensitive. Small artefacts were recognized as printed register marks. As alternative a stroboscope lamp was used. The frequency of the stroboscope is adjusted to the printing speed. Thus the register marks can be checked optically and the servo drives can be regulated in case of a misfit of the register marks.

With the first printing results of the newly developed graphene ink for gravure printing we got

to know that especially the drying of the graphene ink is a challenge. The time for drying was much too long for an in-line process. In principle the drying time can be reduced by using hot air. But the polymer films do not resist high temperatures. Further, for a roll-to-roll printing with a speed of 20-30 m/min this drying method is not sufficient. Thus, an alternative drying method had to be sought. The answer to this problem was near infrared drying. Polymer films used in this project (e.g. PET) do hardly absorb NIR-radiation (Figure 35). Thus, they are almost transparent for the NIR-radiation and the polymer films are hardly thermally stressed. On the other side black graphene ink absorbs NIR-radiation very well. In the laboratory of a drying specialist several tests with NIR-drying were performed. With this drying technique the graphene ink could be dried in a very short time suitable for a roll-to-roll process. Two NIR drying modules were ordered, one for each printing unit of the two-colour printing machine. If needed the power of the NIR emitters can be reduced by the control unit. But it must be considered that the spectrum of a reduced emitter is shifted compared to the full power.

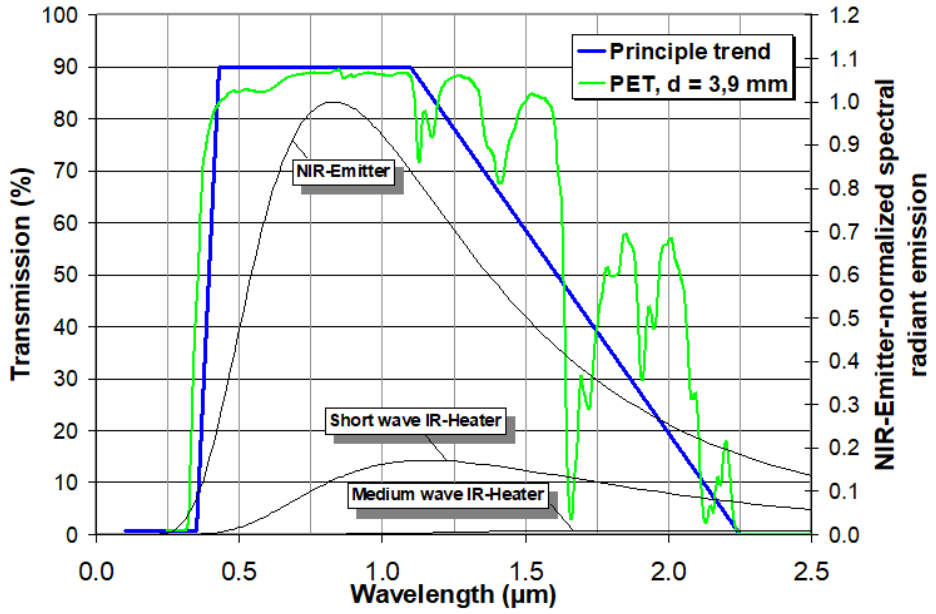

Figure 35: Normalised spectral radiant emission, source Adphos Digital Printing GmbH.

Especially the electromechanical construction and the programming of the control unit were very time-consuming. But finally a fully functional roll-to-roll production line for efficient surface functionalization in a two-colour printing process was available (Figure 36). The results concerning the developed two-colour printing machine were published in wt Werkstattstechnik online (2017) [19].

After implementation of the new roll-to-roll printing machine it turned out that the printed graphene structures absorbed the NIR-radiation of the drying module so well that a too high amount of energy was transferred to the polymer film underneath and the polymer film began to crinkle. To solve this, the machine was modified so that the printing speed could be increased to 40 m/min. At this higher speed the impact of the NIR-radiation on the polymer film was reduced. However, this higher speed led to an insufficient drying of the proteins due to the shorter NIR exposure time. Thus, in the second drying module the NIR-emitters were exchanged. The new emitters are of higher power and the drying of the proteins is ensured.

Figure 36: New two-colour roll-to-roll printing machine, source SAUERESSIG GmbH + Co. KG.

4 Summary of results and possible applications

4.1 Summary of the results

The objectives mentioned in the project description and going beyond the state of the art were achieved during the project period. This extended the state of the art.

The demonstrator of a roll-to-roll production machine is available to mass-produce printed impedimetric sensors with graphene electrodes.

There is a graphene ink available, which was shown by cytotoxicity tests according to DIN ISO 10993-5 as not cytotoxic. Depending on the composition, the ink has a square resistance of < 10 Ω/sq (based on a layer thickness of 25 µm). The graphene ink is suitable for the printing of interdigital electrodes in rotary gravure printing. The size of the smallest printed structures was 50 µm. The printing of smaller structures seems not to be promising because the graphene flakes used have lateral dimensions of up to about 20 µm and therefore are not compatible with well widths in the printing cylinder, which are below 50 µm.

A protein ink based on Matrigel is available and suitable for rotary gravure printing. Printed layers have a thickness of about 4 to 5 µm, adhere to printed graphene structures and do not increase the measured impedance of coated interdigital electrodes. It was shown that the protein coating increases cell adhesion on the electrodes.

A roll-to-roll process for the surface functionalization of large-area polymer films by printing a microstructured graphene / protein layer sequence in a gravure printing process by using a two-colour printing machine is present. An alternative process for manually coating printed graphene structures with Matrigel was also developed.

Sensors for online monitoring of the virus-induced cytopathic effect in cell culture are available. These consist essentially of gravure printed sensors on a polymer film, which is connected by an adhesive bonding process with a bottomless multiwell plate. Online monitoring of the viral effect on the cell culture and of the inhibition of the virus-induced cytopathic effect by antiviral substances is possible with the help of the developed sensors. Furthermore, printed sensors for performing repeated dose experiments over 28 days are available and successfully tested.

4.2 Possible applications

The BIOGRAPHY printing machine and the developed printing and coating processes can be employed in various fields of biotechnology to produce cost-effective and therefore competitive products. SMEs and start-ups are particularly active in modern biotechnology. Their innovativeness and competitiveness are improved by the results of BIOGRAPHY. In bilateral projects with these companies, Fraunhofer IBMT plans to adapt the developed technologies to the special needs of these companies. Specifically, this may mean that Fraunhofer IBMT optimizes processes for the immobilization of graphene or very specific proteins on very specific substrate materials with the existing experimental system and transfers the process parameters to these companies. There are already plans for such cooperation between different partners of the BIOGRAPHY consortium.

The developed impedimetric biosensors in multiwell plate format can be used for many different applications. Examples include (I) virus titer quantification of live viral vaccines (e.g. mumps, measles, rubella), (II) the quantification of neutralizing antibody responses in the field of the development of new promising vaccine candidates (e.g. HIV-1, influenza), (III) industrial screening for new antiviral substances. There is a great need for simple and fast testing procedures.

In addition to the neutralization tests the manufacturing solutions developed in the project open up other application areas in the field of analytics. Particularly young technology companies, which are active in the area of the growth market for point-of-care diagnostics, would benefit from the developed cost-efficient and therefore more competitive roll-to-roll immobilization technology. For example, a roll-to-roll method for graphene coating and surface immobilization of receptor molecules on microfluidic disposable films could be developed based upon the project results.

5 Acknowledgement

This research and development project was funded by the German Federal Ministry of Education and Research (BMBF) within the "Innovations for Tomorrow's Production, Services, and Work" Program and supervised by the Project Management Agency Karlsruhe (PTKA).

The project partners thank the BMBF for the support of the project and the project supervisor. Part of the project work was undertaken in collaboration with UK partners under the M-ERA.NET, an EU funded network. Furthermore, this project is co-funded by Innovate UK. Innovate UK is the UK's innovation agency. It works with people, companies and partner organisations to find and drive the science and technology innovations that will grow the UK economy.

The project partners would like to thank for the support funding.

6 List of references

[1] Singh et al., Inkjet Printing Process and Its Applications. Adv. Mater. 2010, 22, 673–685.

[2] Shimoda et al., Solution-Processed Silicon Films and Transistors. Nature 2006, 440, 783–786.

[3] Noh et al., Ink-jet Printed ZnO Nanowire Field Effect Transistors. Appl. Phys. Lett. 2007, 91, 043109–3.

[4] Okimoto et al., Tunable Carbon Nanotube Thin- Film Transistors Produced Exclusively via Inkjet Printing. Adv. Mater. 2010, 22, 3981–3986.

[5] Singh et al., Inkjet Printing Process and Its Applications. Adv. Mater. 2010, 22, 673–685.

[6] Luechinger et al., Graphene-Stabilized Copper Nanoparticles as an Air-Stable Substitute for Silver and Gold in Low-Cost Ink-Jet Printable Electronics. Nanotechnology 2008, 19, 445201.

[7] Ha et al., Printed, Sub-3V Digital Circuits on Plastic from Aqueous Carbon Nanotube Inks. ACS Nano 2010, 4, 4388–4395.

[8] Torrisi et al., Inkjet-Printed Graphene Electronics, ACSNANO, VOL. 6, NO. 4, 2992–3006, 2012.

[9] Han et al., Scalable, printable, surfactant-free graphene ink directly from graphite, Nanotechnology 24 (2013) 205304 (7pp).

[10] Feil et al., Evaluation of printed microsensors for microphysiometry, 39th Annual International Conference of the IEEE Engineering in Medicine and Biology Society, July 11-15, 2017, Jeju Island, Korea.

[11] https://www.azom.com/article.aspx?ArticleID=15640; retrieved on July 11, 2018.

[12] Knoll et al., High-resolution gravure printing of graphene for biomedical applications, Advanced Functional & Industrial Printing conference (AFIP 2016), 2-3 March 2016, Düsseldorf, Germany.

[13] Knoll et al., High-resolution gravure printing of graphene biosensors, Proceedings of The Global Conference on Micro Manufacture, Incorporating the 11th International Conference on Multi-Material Micro Manufacture (4M) and the 10th International Workshop on Microfactories (IWMF) (4M/IWMF2016), 13-15 September 2016, Kgs. Lyngby, Denmark.

[14] Velten et al., Low-cost biosensors with printed interdigitated graphene electrodes, LOPEC 2018 Conference, March 13-15, 2018, Munich, Germany.

[15] Kleymann et al., New helicase-primase inhibitors as drug candidates for the treatment of herpes simplex disease. Nat. Med. 2002, 8, 392-398.

[16] Biswas et al., Pharmacokinetics-pharmacodynamics of the helicase-primase inhibitor pritelivir following treatment of wild-type or pritelivir-resistant virus infection in a murine herpes

simplex virus 1 infection model. Antimicrob Agents Chemother. 2014, 58, 3843-3852.

[17] Wiest et al., 28-day microphysiological monitoring of human hepatocellular cells, ALTEX Proceedings 4(2), 2015, LINZ 2015, page 254.

[18] Brischwein et al., Microphysiometry, In: Bioanalytical Reviews, Springer, Berlin, Heidelberg. (2018).

[19] Knoll et al., Zweifarben-Druckanlage für die Sensorherstellung, wt-online 11/12-2017, pages 827-833.

Link to the dataset in the database „Fraunhofer-Publica“
http://publica.fraunhofer.de/dokumente/N-503293.html
urn:nbn:de:0011-n-5032931